Exhibit M

GYN-18-1020: Final Decision

Gynecologic Oncology <eesserver@eesmail.elsevier.com>

Wed 9/19/2018 1:26 PM

Deleted Items

To: Ghassan Saed <gsaed@med.wayne.edu>;

Cc: Nicole King <nfletche@med.wayne.edu>; Ira Memaj <ira.memaj@wayne.edu>; Robert Morris <rmorris@med.wayne.edu>; akharp627@gmail.com <akharp627@gmail.com>; Amy Harper <aharper4@med.wayne.edu>; florrie1522@gmail.com <florrie1522@gmail.com>;

Ms. No.: GYN-18-1020
Title: Molecular basis supporting the association of talcum powder use with increased risk of ovarian cancer
Corresponding Author: Dr. Ghassan M. Saed
Authors: Nicole M Fletcher, Ph.D.; Ira Memaj, M.S.; Rong Fan, M.S.; Amy K Harper, M.D.; Robert T Morris, M.D.;

Dear Dr. Saed,

Your paper, referenced above, has now been reviewed by at least two experts in the field and the Editors. Based on the reviewers' comments, we must inform you that while your work is not without merit, we are unable to accept your manuscript for publication in Gynecologic Oncology. In the last year we have seen a significant increase in the number of manuscripts submitted to the Journal and as a result, we are now accepting less than 20% of the manuscripts submitted to the Gynecologic Oncology.

We have attached the comments of the reviewers below in order for you to understand the basis for our decision. We hope that their thoughtful comments will help you in your future studies and possibly, with submission to another journal. Please note that a revised version of the current manuscript should not be submitted for another review to Gynecologic Oncology .

The critique of this paper in no way implies a lack of interest in this area of research, and we invite you to submit your future work to the Journal.

Sincerely,

Robert E. Bristow, MD
Editor
Gynecologic Oncology

Editorial Office
Elsevier

E-mail: gyn@elsevier.com

Reviewers' comments:

Reviewer #1: The stated objective of the study by Fletcher and colleagues is to determine the effects of talc on expression of key inflammatory and redox markers in ovarian cancer and normal cell lines. Normal ovarian and EOC cells were treated with various doses of talc for 48 hours. Levels of CA-125 and selected key redox enzymes were measured using real-time RT-PCR and ELISA.
Overall this is a well-written manuscript and the conclusions are supported by the results. This is an important but controversial topic in need of rigorous scientific inquiry. The current in vitro study does provide novel information, but there are also some important limitations described below:
1. The significance of this study would be greatly enhanced if a mouse model corroborated the cell line findings. In this reviewer's opinion the cell line studies alone and the increase in CA-125 while intriguing are not sufficiently convincing.
2. The significance of SNP alterations should be further clarified
3. The first bulleted highlight, "Oxidative stress is a key mechanism to the initiation and progression of ovarian cancer" is not supported by this investigation and should be omitted.

Reviewer #2: The objective of this study was to investigate the effects of talc on inflammation and redox markers in ovarian cancer and normal cell lines. Talc-treated carcinoma cell lines and normal ovarian cells had a significant dose-dependent increase in the levels of the pro-oxidants inducible nitric oxide synthase (iNOS), nitrate/nitrite and myeloperoxidase (MPO), as well as CA 125, and decrease in the levels of the antioxidants CAT, SOD3, GSR, and GPX. Induction of mutations in key-enzymes affecting their activity was found in talc-treated cells compared to controls.

While the authors compellingly show changes in several key-enzymes regulating redox potential in cells exposed to talc, their data do not show, despite the authors' claim, any evidence that these cells are transformed. Specifically, no experiments documenting changes in cell survival, proliferation or resistance to apoptosis have been performed. Consequently, neither tumor initiation nor progression is documented in this study, as opposed to the statement in Highlight # 1 and elsewhere. While changes in redox potential play an important role in tumor biology in general, the present data are insufficient to back up the claim that talcum is central to the development of ovarian cancer.

Other comments:

The introduction should be better organized, with shorter description of the general features of ovarian cancer, replaced by a brief overview of redox proteins in cancer, followed by a discussion of their role in ovarian cancer.

The fact that SNPs were changed following such short exposure to talcum is surprising and makes one wonder what the biological effect of such changes might be.

References are in inconsistent style, some missing data (e.g. volume and page in # 7)

Exhibit N

Reproductive Sciences

Molecular basis supporting the association of talcum powder use with increased risk of ovarian cancer

Journal:	*Reproductive Sciences*
Manuscript ID	RSCI-18-671
Manuscript Type:	Original Manuscripts
Date Submitted by the Author:	10-Oct-2018
Complete List of Authors:	Fletcher, Nicole; Wayne State University School of Medicine, Obstetrics and Gynecology Harper, Amy; Wayne State University School of Medicine, Obstetrics and Gynecology Memaj, Ira; Wayne State University School of Medicine, Obstetrics and Gynecology Fan, Rong; Wayne State University School of Medicine, Obstetrics and Gynecology Morris, Robert ; Wayne State University School of Medicine, Obstetrics and Gynecology Saed, Ghassan; Wayne State University School of Medicine, Obstetrics and Gynecology
Keyword:	talcum powder, oxidative stress, single nucleotide polymorphism, cell proliferation, epithelial ovarian cancer
File Designation:	

1

Molecular basis supporting the association of talcum powder use with increased risk of ovarian cancer.

Nicole M. Fletcher, Ph.D.[a], Amy K. Harper, M.D.[a], Ira Memaj, B.S.[a], Rong Fan, M.S.[a], Robert T. Morris, M.D.[b], Ghassan M. Saed, Ph.D.[a]

[a]Department of Obstetrics and Gynecology, Wayne State University School of Medicine and [b]Department of Gynecologic Oncology, Karmanos Cancer Institute, Detroit, MI

Corresponding Author:

Ghassan M. Saed, Ph.D.

Associate Professor of Gynecologic Oncology

Director of Ovarian Cancer Biology Research

Departments of Obstetrics and Gynecology and Oncology

Member of Tumor Biology and Microenvironment Program

Karmanos Cancer Institute

Wayne State University School of Medicine

Detroit, MI 48201

(313) 577-5433 Office phone

(313) 577-8544 Office fax

(313) 577-1302 Lab phone

gsaed@med.wayne.edu

Abstract

Genital use of talcum powder and its associated risk of ovarian cancer is an important controversial topic. Epithelial ovarian cancer (EOC) cells are known to manifest a persistent pro-oxidant state. Here we demonstrated that talc induces significant changes in key redox enzymes and enhances the pro-oxidant state in normal and EOC cells. Using real-time RT-PCR and ELISA, levels of CA-125, caspase-3, nitrate/nitrite, and selected key redox enzymes, including myeloperoxidase (MPO), inducible nitric oxide synthase (iNOS), superoxide dismutase (SOD), catalase (CAT), glutathione peroxidase (GPX) and glutathione reductase (GSR) were determined. TaqMan® Genotype analysis utilizing the QuantStudio 12K Flex was used to assess single nucleotide polymorphisms in genes corresponding to target enzymes. Cell proliferation was determined by MTT Proliferation Assay. In all talc treated cells, there was a significant dose-dependent increase in pro-oxidants iNOS, nitrate/nitrite, and MPO with a concomitant decrease in anti-oxidants CAT, SOD, GSR, and GPX ($p<0.05$). Remarkably, talc exposure induced specific point mutations that are known to alter the activity in some of these key enzymes. Talc exposure also resulted in a significant increase in inflammation as determined by increased tumor marker CA-125 ($p<0.05$). More importantly, talc exposure significantly induced cell proliferation and decreased apoptosis in cancer cells and to greater degree in normal cells ($p<0.05$). These findings are the first to confirm the cellular effect of talc and provide a molecular mechanism to previous reports linking genital use to increased ovarian cancer risk.

Keywords: talc, epithelial ovarian cancer, oxidative stress, single nucleotide polymorphism, cell proliferation

Introduction

Ovarian cancer is the most lethal gynecologic malignancy and ranks fifth in cancer deaths among women diagnosed with cancer[1]. Epithelial ovarian cancer (EOC) has long been considered a

heterogeneous disease with respect to histopathology, molecular biology, and clinical outcome[1, 2]. It comprises at least five distinct histological subtypes, the most common and well-studied being high-grade serous ovarian cancer. Although surgical techniques and treatments have advanced over the years, the prognosis of EOC remains poor, with a 5-year survival rate of 50% in advanced stage[2]. This is largely due to the lack of early warning symptoms and screening methods, and the development of chemoresistance[1, 2]. Moreover, ovarian cancer is known to be associated with germline mutations in the BRCA1 or BRCA2 genes, but with a rate of only 20-40%, this suggests the presence of other unknown mutations in other predisposition genes[3]. Additional genetic variations including single nucleotide polymorphisms (SNPs) have been hypothesized to act as low to moderate penetrant alleles that contribute to ovarian cancer risk[3, 4]. Non-synonymous SNPs substitute encoded amino acids in proteins and are more likely to alter the structure, function, and interaction of the protein[4].

The pathophysiology of EOC is not fully understood but has been strongly associated with inflammation and the resultant oxidative stress[5]. We have previously characterized EOC cells to manifest a persistent pro-oxidant state as evident by the upregulation of key oxidants and downregulation of key antioxidants. This redox state is further enhanced in chemoresistant EOC cells[6]. The expression of key pro-oxidant/inflammatory enzymes such as inducible nitric oxide synthase (iNOS), nicotinamide adenine dinucleotide phosphate (NAD(P)H) oxidase, and myeloperoxidase (MPO), as well as an increase in nitric oxide (NO) levels were increased in EOC tissues and cells[7]. Additionally, we have shown that EOC cells manifest lower apoptosis, which was markedly induced by inhibiting iNOS, indicating a strong link between apoptosis and NO/iNOS pathways in these cells[7].

The cellular redox balance is maintained by key antioxidants including catalase (CAT), superoxide dismutase (SOD) or by glutathione peroxidase (GPX) coupled with glutathione reductase (GSR)[5]. Other important scavengers include thioredoxin coupled with thioredoxin reductase, and glutaredoxin, which utilizes glutathione (GSH) as a substrate[7]. We have previously reported that a genotype switch in key antioxidants is a potential mechanism leading to the acquisition of

chemoresistance in EOC cells[7]. We have studied the effects of genetic polymorphisms in key redox genes on the acquisition of the oncogenic phenotype in EOC cells. Functional polymorphisms in genes that control the levels of cellular ROS and oxidative damage, including SNPs for genes involved in carcinogen metabolism (detoxification and/or activation), antioxidants, and DNA repair pathways were tested[4, 7]. Several function-altering SNPs have been identified in key antioxidants, including CAT, GPX, GSR, and SOD[4].

Several studies have suggested the possible association between genital use of talcum powder and risk of EOC[7-9]. Association between the use of cosmetic talc in genital hygiene and ovarian cancer was first described in 1982 by Cramer, et al, and many subsequent studies found talc use to increase risk for ovarian cancer[7]. Talc and asbestos are both silicate minerals; the carcinogenic effects of asbestos have been extensively studied and documented in the medical literature[7, 8]. Asbestos fibers in the lung initiate an inflammatory and scarring process, and it has been proposed that ground talc, as a foreign body, might initiate a similar inflammatory response[7]. The objective of this study was to determine the effects of talcum powder on the expression of key redox enzymes, CA-125 levels, and cell proliferation and apoptosis in normal and EOC cells.

Material and Methods

Cell Lines. Ovarian cancer cells SKOV-3 (ATCC), A2780 (Sigma Aldrich, St. Louis, MO), and TOV112D (a kind gift from Gen Sheng Wu at Wayne State University, Detroit, MI) and normal cells human macrophages (EL-1, ATCC, Manassas, VA), human primary normal ovarian epithelial cells (Cell Biologics, Chicago, IL), human ovarian epithelial cells (HOSEpiC, ScienCell Research Laboratories, Inc., Carlsbad, CA), immortalized human fallopian tube secretory epithelial cells (FT33, Applied Biological Materials, Richmond, BC, Canada) were used. All cells were grown in media and conditions following manufacturer's protocol. EL-1 cells were grown in IMDM media (ATCC) supplemented with 0.1 mM hypoxanthine and 0.1 mM thymidine solution (H-T, ATCC) and 0.05mM β-mercaptoethanol. SKOV-3 EOC cells were grown in HyClone McCoy's 5A medium (Fisher Scientific, Waltham, MA), A2780 EOC

cells were grown in HyClone RPMI-1640 (Fisher Scientific), and both TOV112D EOC cells were grown in MCDB105 (Cell Applications, San Diego, CA) and Medium 199 (Fisher Scientific) (1:1). All media was supplemented with fetal bovine serum (FBS, Innovative Research, Novi, MI) and penicillin/streptomycin (Fisher Scientific), per their manufacturer specifications. Human primary normal ovarian epithelial cells were grown in Complete Human Epithelial Cell Medium (Cell Biologics).

Treatment of cells. Talcum powder (Fisher Scientific, Catalog #T4-500, Lot#166820) or baby powder (Johnson & Johnson, #30027477, Lot#13717RA) was dissolved in DMSO (Sigma Aldrich) at a concentration of 500 mg in 10 ml and was filtered with a 0.2 µm syringe filter (Corning). Sterile DMSO was used as a control for all treatments. Cells were seeded in 100 mm cell culture dishes (3×10^6) and were treated 24 hours later with 5, 20, or 100 µg/ml of talc for 48 hours. Cell pellets were collected for RNA, DNA, and protein extraction. Cell culture media was collected for CA-125 analysis by ELISA.

Real-Time RT-PCR. Total RNA was extracted from all cells using the RNeasy Mini Kit (Qiagen, Valencia, CA) according to the protocol provided by the manufacturer. Measurement of the amount of RNA in each sample was performed using a Nanodrop Spectrophotometer (Thermo Fisher Scientific, Waltham, MA). A 20 µL cDNA reaction volume containing 0.5 µg RNA was prepared using the SuperScript VILO Master Mix Kit (Life Technologies, Carlsbad, CA), as described by the manufacturer's protocol. Optimal oligonucleotide primer pairs were selected for each target using Beacon Designer (Premier Biosoft, Inc., Table 1). Quantitative RT-PCR was performed using the EXPRESS SYBR GreenER qPCR Supermix Kit (Life Technologies) and the Cepheid 1.2f Detection System as previously described [6]. Standards with known concentrations and lengths were designed specifically for *β-actin* (79 bp), *CAT* (105 bp), *NOS2* (89 bp), *GSR* (103 bp), *GPX1* (100 bp), *MPO* (79 bp), and *SOD3* (84 bp), allowing for construction of a standard curve using a 10-fold dilution series[6]. A specific standard for each gene allows for absolute quantification of the gene in number of copies, which can then be expressed per microgram of RNA. All samples were normalized to the housekeeping gene, *β-actin*. A final melting curve analysis was performed to demonstrate specificity of the PCR product.

Protein Detection. Cell pellets were lysed utilizing cell lysis buffer (20 mM Tris-HCl (pH 7.5), 150 mM NaCl, 1 mM Na2EDTA, 1 mM EGTA, 1% Triton, 2.5 sodium pyrophosphate, 1 mM beta-glycerophosphate, 1 mM Na3VO4, 1 µg/ml leupeptin) containing a cocktail of protease inhibitors. Samples were centrifuged at 13000 rpm for 10 minutes at 4°C. Total protein concentration of cell lysates from control and talc treated cells was measured with the Pierce BCA Protein Assay Kit (Thermo Scientific, Rockford, IL) per the manufacturer's protocol.

Detection of Protein/Activity by ELISA. ELISA kits for each target were purchased and used according to the manufacturer's protocol. The following ELISA kits were purchased from Cayman Chemical (Ann Arbor, MI): CAT, SOD, GSR, GPX, and MPO. Nitrite (NO_2^-)/nitrate (NO_3^-) were determined spectrophotometrically by measuring their absorbance at 210 nm after separation by HPLC with standard NO_2^-/NO_3^- as previously reported[6]. The analysis was performed by a HPLC system (Shimadzu Scientific Instruments, Inc.) including a LC-10ADV pump, frc-10A injector and DGU-14A degasser. Nitrite/nitrate was detected using an RF-10 XL fluorescence detector with 210 nm excitation and 440 nm emission. CA-125 protein levels were measured in cell media by ELISA from Ray Biotech (Norcross, GA) according to the manufacturer's protocol.

TaqMan® SNP Genotyping Assay. DNA was isolated utilizing the EZ1 DNA Tissue Kit (Qiagen) for EOC cells according the manufacturer's protocols. The TaqMan® SNP Genotyping Assay Set (Applied Biosystems, Carlsbad, CA) (NCBI dbSNP genome build 37, MAF source 1000 genomes) were used to genotype the SNPs (Table 1). The Applied Genomics Technology Center (AGTC, Wayne State University, Detroit, MI) performed these assays. Analysis was done utilizing the QuantStudioTM 12 K Flex Real-Time PCR System (Applied Biosystems).

Cell Proliferation and Apoptosis. Cell proliferation was assessed with the TACS MTT Cell Proliferation Assay (Trevigen, Gaithersburg, MD) per the manufacturer's protocol after treatment with talc (100 µg/mL) for 48 hours. The Caspase-3 Colorimetric Activity Assay Kit (Chemicon, Temecula, CA) was used to determine levels of caspase-3 activity after treatment of

normal and EOC cells with various doses of talc as previously described[7]. Equal concentrations of cell lysate were used. The assay is based on spectrophotometric detection of the chromophore p-nitroaniline (pNA) after cleavage from the labeled substrate DEVD-pNA. The free pNA can be quantified using a spectrophotometer or a microtiter plate reader at 405 nm. Comparison of the absorbance of pNA from an apoptotic sample with its control allows determination of the percent increase in caspase-3 activity.

Statistical Analysis. Normality was examined using the Kolmogorov-Smirnov test and by visual inspection of quantile-quantile plots. Because most of the data were not normally distributed, differences in distributions were examined using the Kruskal-Wallis test. Generalized linear models were fit to examine pairwise differences in estimated least squares mean expression values by exposure to 0, 5, 20 or 100 µg/ml of talc. We used the Tukey-Kramer adjustment for multiple comparisons, and the regression models were fit using log2 transformed analyte expression values after adding a numeric constant '1' to meet model assumptions while avoiding negative transformed values. P-values below 0.05 are statistically significant.

Results

Talc treatment decreased the expression of antioxidant enzymes SOD and CAT in normal and EOC cells. Real-time RT-PCR and ELISA assays were utilized to determine the CAT and SOD mRNA and protein levels in cells before and after 48 hours talc treatment, respectively (Figure 1). CAT mRNA and protein levels were significantly decreased in a dose-dependent manner in talc treated cells compared to controls (Figure 1. A, C, $p<0.05$). Similarly, SOD mRNA and protein levels were significantly decreased in a dose- dependent manner in talc treated cells compared to controls (Figure 1. B, D, $p<0.05$).

Talc treatment increased the expression of prooxidants iNOS, NO_2^-/NO_3^- and MPO in normal and EOC cells. Real-time RT-PCR and NO_2^-/NO_3^- assays were utilized to determine the iNOS mRNA and NO levels in cells before and after 48 hours talc treatment, respectively (Figure 2). iNOS mRNA and NO

levels were significantly increased in a dose-dependent manner in talc treated cells as compared to their controls (Figure 2. A, C, $p<0.05$). As expected, there was no detectable MPO in normal ovarian and fallopian tube cells, and thus talc treatment did not have any effect. However, MPO mRNA and protein levels were significantly increased in a dose-dependent manner in talc treated ovarian cancer cells and macrophages compared to controls (Figure 2. B, D, $p<0.05$).

Talc treatment decreased the expression of antioxidant enzymes, GPX and GSR in normal and EOC cells. Real-time RT-PCR and ELISA assays were utilized to determine the GPX and GSR mRNA and protein levels in cells before and after 48 hours talc treatment, respectively (Figure 3). GPX mRNA and protein levels were significantly decreased in a dose-dependent manner in talc treated cells compared to controls (Figure 3. A, C, $p<0.05$). Similarly, GSR mRNA and protein levels were significantly decreased in a dose-dependent manner in talc treated cells compared to controls (Figure 3. B, D, $p<0.05$).

Talc exposure induced known genotype switches in key oxidant and antioxidant enzymes. Talc treatment was associated with a genotype switch in *NOS2* from the common C/C genotype in untreated cells to T/T, the SNP genotype, in talc treated cells, except in A2780 and TOV112D (Table 2). Additionally, the observed decrease in CAT expression and activity was associated with a genotype switch from common C/C genotype in CAT in untreated cells to C/T, the SNP genotype, in TOV112D and all normal talc treated cells. However, there was no detectable genotype switch in CAT in A2780, SKOV3, and TOV112D (Table 2). Remarkably, there was no observed genotype switch in the selected SNP for SOD3 and GSR in all talc treated cells. All cells except for HOSEpiC cells manifest the SNP genotype of *GPX1* (C/T). Intriguingly, talc treatment reversed this SNP genotype to the normal genotype (Table 2).

Talc treatment increased CA-125 levels in normal and EOC cells. CA-125 ELISA assay was performed in protein isolated from cell media before and after talc treatment. CA-125 levels were significantly increased in a dose-dependent manner in all cells (Figure 4, $p<0.05$). There was no detectable CA-125 protein in macrophages.

Talc treatment increased cell proliferation and decreased apoptosis. MTT Cell Proliferation Assay was used to determine cell viability, and Caspase-3 Activity assay was utilized to determine apoptosis of all cell lines after 48 hours talc treatment (Figure 5). Cell proliferation was significantly increased from the baseline in all talc treated cells ($p<0.05$), but to a greater degree in normal as compared to cancer cells. As anticipated, caspase-3 was significantly reduced in cancer as compared to normal cells. Talc treatment resulted in decreased caspase-3 activity in all cells as compared to controls (Figure 6, $p<0.05$), indicating a decrease in apoptosis.

Discussion

The claim that regular use of talcum powder for hygiene purpose is associated with an increased risk of ovarian cancer is based on several reports confirming the presence of talc particles in the ovaries and other parts of the female reproductive tract as well as in lymphatic vessels and tissues of the pelvis[7, 8]. A study by Cramer, et al has reported the presence of talc in pelvic lymph nodes of a woman with ovarian cancer who used talc daily for 30 years[7]. The ability of talc particles to migrate through the genital tract to the distal fallopian tube and ovaries is well accepted[7, 8]. To date, the exact mechanism is not fully understood, though several studies have pointed toward the peristaltic pump feature of the uterus and fallopian tubes, which is known to enhance transport of sperm into the oviduct ipsilateral to the ovary bearing the dominant follicle[8-10].

There are reports supporting the epidemiologic association of talc use and risk of ovarian cancer[11, 12]. Recent studies have shown that risks for EOC from genital talc use vary by histologic subtype, menopausal status at diagnosis, hormone therapy use, weight, and smoking. These observations suggest that estrogen and/or prolactin may play a role via macrophage activity and inflammatory response to talc. There has been debate as to the significance of the epidemiologic studies based on the fact that the reported epidemiologic risk of talc use and risk of ovarian cancer, although consistent, is relatively modest (30-40%), and there is inconsistent increase in risk with duration of use. This observation is due,

in part, to the challenges in quantifying exposure as well as the failure of epidemiological studies to obtain necessary information about the frequency and duration of usage[11-13].

In this study, we have shown beyond doubt that talc alters key redox and inflammatory markers, enhances cell proliferation, and inhibits apoptosis, which are hallmarks of ovarian cancer. More importantly, this effect is also manifested by talc in normal cells, including surface ovarian epithelium, fallopian tube, and macrophages. Oxidative stress has been implicated in the pathogenesis of ovarian cancer, specifically, by increased expression of several key pro-oxidant enzymes such as iNOS, MPO, and NAD(P)H oxidase in EOC tissues and cells as compared to normal cells indicating an enhanced redox state, as we have recently demonstrated[14]. This redox state is further enhanced in chemoresistant EOC cells as evident by a further increase in iNOS and $NO2^-/NO3^-$ and a decrease in GSR levels, suggesting a shift towards a pro-oxidant state[14]. Antioxidant enzymes, key regulators of cellular redox balance, are differentially expressed in various cancers, including ovarian[14, 15]. Specifically, GPX expression is reduced in prostate, bladder, and estrogen receptor negative breast cancer cell lines as well as in cancerous tissues from the kidney. However, GPX activity is increased in cancerous tissues from breast[15]. Glutathione reductase levels, on the other hand, are elevated in lung cancer, although differentially expressed in breast and kidney cancerous tissues[5, 16]. Similarly, CAT was decreased in breast, bladder, and lung cancer while increased in brain cancer[17-19]. Superoxide dismutase is expressed in lung, colorectal, gastric ovarian, and breast cancer, while decreased activity and expression have been reported in colorectal carcinomas and pancreatic cancer cells[19-22]. Collectively, this differential expression of antioxidants demonstrates the unique and complex redox microenvironment in cancer. Glutathione reductase is a flavoprotein that catalyzes the NADPH-dependent reduction of oxidized glutathione (GSSG) to GSH. This enzyme is essential for the GSH redox cycle which maintains adequate levels of reduced cellular GSH. A high GSH/GSSG ratio is essential for protection against oxidative stress (Figure 5). Treatment with talc significantly reduced GSR in normal and cancer cells, altering the redox balance (Figure 3. A, C). Likewise, GPX is an enzyme that detoxifies reactive electrophilic intermediates and thus

plays an important role in protecting cells from cytotoxic and carcinogenic agents. Overexpression of GPX is triggered by exogenous chemical agents and reactive oxygen species, and is thus thought to represent an adaptive response to stress[16]. Indeed, treatment of normal and cancer cells with talc significantly reduced GPX, which compromised the overall cell response to stress (Figure 3. B, D).

We have previously reported that EOC cells manifest increased cell proliferations and decreased apoptosis[14]. In this study, we have shown that talc enhances cell proliferation and induces an inhibition in apoptosis in EOC cells, but more importantly in normal cells, suggesting talc is a stimulus to the development of the oncogenic phenotype. We also previously reported a cross-talk between iNOS and MPO in ovarian cancer which contributed to the lower apoptosis observed in ovarian cancer cells[14, 23]. Myeloperoxidase, an abundant hemoprotein, previously known to be present solely in neutrophils and monocytes, is a key oxidant enzyme that utilizes NO produced by iNOS as a one-electron substrate generating NO^+, a labile nitrosylating species[14, 24, 25]. Indeed, we were the first to report that MPO was expressed by EOC cells and tissues[23]. Silencing MPO gene expression utilizing MPO specific siRNA induced apoptosis in EOC cells through a mechanism that involved the S-nitrosylation of caspase-3 by MPO[23]. Additionally, we have compelling evidence that MPO serves as a source of free iron under oxidative stress, where both NO^+ and superoxide are elevated[14]. Iron reacts with hydrogen peroxide (H_2O_2) and catalyzes the generation of highly reactive hydroxy radical ($HO^\bullet$), thereby increasing oxidative stress, which in turn increases free iron concentrations by the Fenton and Haber–Weiss reaction[14, 25]. We have previously highlighted the potential benefits of the combination of serum MPO and free iron as biomarkers for early detection and prognosis of ovarian cancer[26]. Collectively, we now have substantial evidence demonstrating that altered oxidative stress may play a role in maintaining the oncogenic phenotype of EOC cells. Treatment of normal or ovarian cancer cells with talc resulted in a significant increase in MPO and iNOS, supporting the role of talc in the enhancement of a pro-oxidant state that is a major cause in the development and maintenance of the oncogenic phenotype (Figure 2).

Furthermore, CA-125, which exists as a membrane-bound and secreted protein in epithelial ovarian cancer cells, has been established as a biomarker for disease progression and response to treatment[2]. CA-125 expression was significantly increased from nearly undetectable levels in controls to values approaching clinical significance (35 U/ml in postmenopausal women[27]) in talc treated cell lines (Figure 4, $p<0.05$) without the physiologic effects on the tumor microenvironment one would expect to be present in the human body, highlighting the implications of the pro-oxidant states caused by talc alone.

To elucidate the mechanism by which talc alters the redox balance to favor a pro-oxidant state not only in ovarian cancer cells, but more importantly in normal cells, we have examined selected known gene mutations in key oxidant and antioxidant enzymes. These mutations correspond to specific SNPs that are known to be associated with altered enzymatic activity and increased cancer risk[6, 28]. Our results show that the *CAT* SNP (rs769217) which results in decreased enzymatic activity was induced in all normal cell lines tested and in TOV112D EOC lines. However, the *CAT* mutation was not detected in A2780 or SKOV-3 cell lines (Table 2). Nevertheless, our results confirm a decrease in CAT expression and enzymatic activity in all talc treated cells (Figure 1), indicating the existence of other *CAT* SNPs. However, the *SOD3* (rs2536512) and *GSR* (rs8190955) SNP genotypes were not detected in any cell line, yet SOD3 and GSR activity and expression were decreased in all talc treated cells, again suggesting the presence of other SNPs. Our results have also shown that all cells, except for HOSEpiC cells, manifest the SNP genotype of *GPX1* (C/T) before talc treatment. Intriguingly, talc treatment reversed this SNP genotype to the normal genotype (Table 2). Consistent with this finding, we have previously reported that acquisition of chemoresistance by ovarian cancer cells is associated with a switch from the *GPX1* SNP genotype to the normal *GPX1* genotype[6]. It is not understood why a *GPX1* SNP genotype predominates in untreated normal and ovarian cancer cells. Additionally, our results showed that talc treatment was associated with a genotype switch from common C/C genotype in *NOS2* in untreated cells to T/T, the SNP genotype, in talc treated cells, except in A2780 and TOV112D (Table 2). Nevertheless, our results confirm an increase in iNOS expression and enzymatic activity in all talc treated cells (Figure 2), again

suggesting the existence of other *NOS2* SNPs. Collectively, these findings support the notion that talc treatment induced gene point mutations that happen to correspond to SNPs in locations with functional effects, thus altering overall redox balance for the initiation and development of ovarian cancer. Future studies examining such SNPs are important to fully elucidate a genotype switch mechanism induced by talc exposure.

In summary, this is the first study to clearly demonstrate that talc induces inflammation and alters the redox balance favoring a pro-oxidant state in normal and EOC cells. We have shown a dose-dependent significant increase in key pro-oxidants, iNOS, $NO2^-/NO3^-$, and MPO and a concomitant decrease in key antioxidant enzymes, CAT, SOD, GPX, and GSR, in all talc treated cells (both normal and ovarian cancer) compared to their controls. Additionally, there was a significant increase in CA-125 levels in all the talc treated cells compared to their controls, except in macrophages. The mechanism by which talc alters the cellular redox and inflammatory balance involves the induction of specific mutations in key oxidant and antioxidant enzymes that correlate with alterations in their activities. The fact that these mutations happen to correspond to known SNPs of these enzymes indicate a genetic predisposition to developing ovarian cancer with genital talcum powder use.

Acknowledgements

Special thanks to Imaan Singh for her technical contributions in acquiring the data and in development of graphics.

Conflict of Interest

The authors declare that there are no conflicts of interest.

References

1. Berek JS, Bertelsen K, du Bois A, et al. [Epithelial ovarian cancer (advanced stage): consensus conference (1998)]. Gynecologie, obstetrique & fertilite. 2000 Jul-Aug;**28**(7-8):576-83.

2. Jelovac D, Armstrong DK. Recent progress in the diagnosis and treatment of ovarian cancer. CA: a cancer journal for clinicians. 2011 May-Jun;**61**(3):183-203.

3. Prat J, Ribe A, Gallardo A. Hereditary ovarian cancer. Hum Pathol. 2005 Aug;**36**(8):861-70.

4. Ramus SJ, Vierkant RA, Johnatty SE, et al. Consortium analysis of 7 candidate SNPs for ovarian cancer. Int J Cancer. 2008 Jul 15;**123**(2):380-8.

5. Reuter S, Gupta SC, Chaturvedi MM, Aggarwal BB. Oxidative stress, inflammation, and cancer: how are they linked? Free Radic Biol Med. 2010 Dec 1;**49**(11):1603-16.

6. Fletcher NM, Belotte J, Saed MG, et al. Specific point mutations in key redox enzymes are associated with chemoresistance in epithelial ovarian cancer. Free Radic Biol Med. 2016 Nov 25;**102**:122-32.

7. Saed GM, Diamond MP, Fletcher NM. Updates of the role of oxidative stress in the pathogenesis of ovarian cancer. Gynecologic oncology. 2017 Jun;**145**(3):595-602.

8. Kunz G, Beil D, Deiniger H, Einspanier A, Mall G, Leyendecker G. The uterine peristaltic pump. Normal and impeded sperm transport within the female genital tract. Adv Exp Med Biol. 1997;**424**:267-77.

9. Leyendecker G, Kunz G, Herbertz M, et al. Uterine peristaltic activity and the development of endometriosis. Ann N Y Acad Sci. 2004 Dec;**1034**:338-55.

10. Zervomanolakis I, Ott HW, Hadziomerovic D, et al. Physiology of upward transport in the human female genital tract. Ann N Y Acad Sci. 2007 Apr;**1101**:1-20.

11. Terry KL, Karageorgi S, Shvetsov YB, et al. Genital powder use and risk of ovarian cancer: a pooled analysis of 8,525 cases and 9,859 controls. Cancer Prev Res (Phila). 2013 Aug;**6**(8):811-21.

12. Penninkilampi R, Eslick GD. Perineal Talc Use and Ovarian Cancer: A Systematic Review and Meta-Analysis. Epidemiology. 2018 Jan;**29**(1):41-9.

13. Reid BM, Permuth JB, Sellers TA. Epidemiology of ovarian cancer: a review. Cancer Biol Med. 2017 Feb;**14**(1):9-32.

14. Saed GM, Diamond MP, Fletcher NM. Updates of the role of oxidative stress in the pathogenesis of ovarian cancer. Gynecologic oncology. 2017 Feb 23.

15. Brigelius-Flohe R, Kipp A. Glutathione peroxidases in different stages of carcinogenesis. Biochimica et biophysica acta. 2009 Nov;**1790**(11):1555-68.

16. Sun Y. Free radicals, antioxidant enzymes, and carcinogenesis. Free Radic Biol Med. 1990;**8**(6):583-99.

17. Popov B, Gadjeva V, Valkanov P, Popova S, Tolekova A. Lipid peroxidation, superoxide dismutase and catalase activities in brain tumor tissues. Arch Physiol Biochem. 2003 Dec;**111**(5):455-9.

18. Ray G, Batra S, Shukla NK, et al. Lipid peroxidation, free radical production and antioxidant status in breast cancer. Breast Cancer Res Treat. 2000 Jan;**59**(2):163-70.

19. Chung-man Ho J, Zheng S, Comhair SA, Farver C, Erzurum SC. Differential expression of manganese superoxide dismutase and catalase in lung cancer. Cancer Res. 2001 Dec 1;**61**(23):8578-85.

20. Radenkovic S, Milosevic Z, Konjevic G, et al. Lactate dehydrogenase, catalase, and superoxide dismutase in tumor tissue of breast cancer patients in respect to mammographic findings. Cell Biochem Biophys. 2013 Jun;**66**(2):287-95.

21. Hu Y, Rosen DG, Zhou Y, et al. Mitochondrial manganese-superoxide dismutase expression in ovarian cancer: role in cell proliferation and response to oxidative stress. J Biol Chem. 2005 Nov 25;**280**(47):39485-92.

22. Svensk AM, Soini Y, Paakko P, Hiravikoski P, Kinnula VL. Differential expression of superoxide dismutases in lung cancer. Am J Clin Pathol. 2004 Sep;**122**(3):395-404.

23. Saed GM, Ali-Fehmi R, Jiang ZL, et al. Myeloperoxidase serves as a redox switch that regulates apoptosis in epithelial ovarian cancer. Gynecologic oncology. 2010 Feb;**116**(2):276-81.

24. Galijasevic S, Saed GM, Hazen SL, Abu-Soud HM. Myeloperoxidase metabolizes thiocyanate in a reaction driven by nitric oxide. Biochemistry. 2006 Jan 31;**45**(4):1255-62.

25. Galijasevic S, Maitra D, Lu T, Sliskovic I, Abdulhamid I, Abu-Soud HM. Myeloperoxidase interaction with peroxynitrite: chloride deficiency and heme depletion. Free Radic Biol Med. 2009 Aug 15;**47**(4):431-9.

26. Fletcher NM, Jiang Z, Ali-Fehmi R, et al. Myeloperoxidase and free iron levels: potential biomarkers for early detection and prognosis of ovarian cancer. Cancer Biomark. 2011;**10**(6):267-75.

27. Scholler N, Urban N. CA125 in ovarian cancer. Biomark Med. 2007 Dec;**1**(4):513-23.

28. Belotte J, Fletcher NM, Saed MG, et al. A Single Nucleotide Polymorphism in Catalase Is Strongly Associated with Ovarian Cancer Survival. PloS one. 2015;**10**(8):e0135739.

Table Legends:

Table 1. Real-time RT-PCR oligionucleotide primers.

Table 2. SNP characteristics (A) and SNP genotyping of key redox enzymes in untreated and talc treated (100 µg/mL) human primary ovarian epithelial cells (Normal ovarian), Human Ovarian Surface Epithelial Cells (HOSEpiC) , fallopian tube (FT33), and ovarian cancer (A2780, SKOV-3, TOV112D) cell lines (B).

Figure Legends:

Figure 1. Decreased expression and activity of key antioxidant enzymes, CAT and SOD3. The mRNA (real-time RT-PCR) and protein/activity levels (ELISA) of CAT (A&C) and SOD3 (B&D) were determined in macrophages (EL-1), human primary ovarian epithelial cells (Normal ovarian), fallopian tube (FT33), and ovarian cancer (SKOV-3, TOV112D, and A2780) cell lines before and after treatment with various doses of talc over 48 hours. Experiments were performed in triplicate. Expression is depicted as the mean with error bars representing standard deviation. All changes in response to talc treatment were significant ($p<0.05$) in all cells and in all doses as compared to controls.

17

Figure 2. Increased expression and activity of key pro-oxidants, iNOS, NO_2^-/NO_3^-, and MPO. The mRNA (real-time RT-PCR) and protein/activity levels (ELISA) of iNOS (A&C) and MPO (B&D) were determined in macrophages (EL-1), human primary ovarian epithelial cells (Normal ovarian), fallopian tube (FT33), and ovarian cancer (SKOV-3, TOV112D, and A2780) cell lines before and after treatment with various doses of talc over 48 hours. As expected, there was no detectable MPO in normal ovarian and fallopian tube cells, and thus talc treatment did not have any effect. Experiments were performed in triplicate. Expression is depicted as the mean with error bars representing standard deviation. All changes in response to talc treatment were significant ($p<0.05$) in iNOS and MPO positive cells and in all doses as compared to controls.

Figure 3. Decreased expression and activity of key antioxidant enzymes, GSR and GPX. The mRNA (real-time RT-PCR) and protein/activity levels (ELISA) of GSR (A&C) and GPX (B&D) were determined in macrophages (EL-1), human primary ovarian epithelial cells (Normal ovarian), fallopian tube (FT33), and ovarian cancer (SKOV-3, TOV112D, and A2780) cell lines before and after treatment with various doses of talc over 48 hours. Experiments were performed in triplicate. Expression is depicted as the mean with error bars representing standard deviation. All changes in response to talc treatment were significant ($p<0.05$) in all cells and in all doses as compared to controls.

Figure 4. Increased CA125 levels in response to talc treatment. The level of ovarian cancer biomarker CA-125 was determined by ELISA before and after 48 hours of talc treatment (100 µg/ml) in macrophages (EL-1), human primary ovarian epithelial cells (Normal ovarian), fallopian tube (FT33), and ovarian cancer (SKOV-3, TOV112D, and A2780) cells. Experiments

were performed in triplicate. Expression is depicted as the mean with error bars representing standard deviation. All changes in response to talc treatment were significant ($p<0.05$) in all cells as compared to controls.

Figure 5. Increased cell proliferation in response to talc treatment. Cell proliferation was determined by MTT Cell Proliferation Assay after 48 hours of talc treatment (100 µg/ml) in macrophages (EL-1), human primary ovarian epithelial cells (Normal ovarian), fallopian tube (FT33), and ovarian cancer (SKOV-3, TOV112D, and A2780) cells. Experiments were performed in triplicate. Cell proliferation is depicted as the mean with error bars representing standard deviation. All changes in response to talc treatment were significant ($p<0.05$) in all cells as compared to controls.

Figure 6. Decreased apoptosis in response to talc treatment. Caspase-3 activity was used to measure the degree of apoptosis in all cells. Caspase-3 Activity Assay was utilized to determine caspase-3 activity in macrophages (EL-1), human primary ovarian epithelial cells (Normal ovarian), fallopian tube (FT33), and ovarian cancer (SKOV-3, TOV112D, and A2780) cell lines before and after treatment with various doses of talc over 48 hours. Experiments were performed in triplicate. Expression is depicted as the mean with error bars representing standard error. All changes in response to talc treatment were significant ($p<0.05$) in all cells and in all doses as compared to controls.

Figure 7. Epithelial ovarian cancer (EOC) cells have been reported to manifest a persistent pro-oxidant state as evident by the upregulation (green arrows) of key oxidants iNOS, NO, NO+,

ONOO-, OH-, O2+, and MPO (blue) and downregulation (red arrows) of key antioxidants SOD, CAT, GPX, and GSR (orange). This redox state was also shown to be further enhanced in chemoresistant EOC cells. In this study, talcum powder altered the redox state, as indicated by the arrows, of both normal and EOC cells to create an enhanced pro-oxidant state.

Accession Number	Gene	Sense (5'-3')	Antisense (3'-5')	Amplicon (bp)	Annealing Time (sec) and Temperature (°C)
NM_001101	*β-actin*	ATGACTTAGTTGCGTTACAC	AATAAAGCCATGCCAATCTC	79	10, 64
NM_001752	*CAT*	GGTTGAACAGATAGCCTTC	CGGTGAGTGTCAGGATAG	105	10, 63
NM_003102	*SOD3*	GTGTTCCTGCCTGCTCCT	TCCGCCGAGTCAGAGTTG	84	60, 64
NM_000637	*GSR*	TCACCAAGTCCCATATAGAAATC	TGTGGCGATCAGGATGTG	116	10, 63
NM_000581	*GPX1*	GGACTACACCCAGATGAAC	GAGCCCTTGCGAGGTGTAG	91	10, 66
NM_000625	*NOS2*	GAGGACCACATCTACCAAGGAGGAG	CCAGGCAGGCGGAATAGG	89	30, 59
NM_000250	*MPO*	CACTTGTATCCTCTGGTTCTTCAT	TCTATATGCTTCTCACGCCTAGTA	79	60, 63

A	Gene (rs number)				
	CAT (rs769217)	*NOS2* (rs2297518)	*GSR* (rs8190955)	*GPX1* (rs3448)	*SOD3* (rs2536512)
MAF	0.123	0.173	0.191	0.176	0.476
SNP	C-262T	C2087T	G201T	C-1040T	A377T
Chromosome Location	11p13	17q11.2	8p12	3q21.31	4p15.2
Amino Acid Switch	Isoleucine to Threonine	Serine to Leucine	Unknown	Proline to Leucine	Alanine to threonine
Effect on Activity	Decrease	Increase	Unknown	Decrease	Decrease

B	Gene (rs number) and Enzyme Activity									
Cell Lines	*CAT* (rs769217)	CAT Activity	*NOS2* (rs2297518)	iNOS Activity	*GSR* (rs8190955)	GSR Activity	*GPX1* (rs3448)	GPX Activity	*SOD3* (rs2536512)	SOD Activity
A2780- Control	C/C	↓ (67%)	C/C	↑ (135%)	G/G	↓ (61%)	C/T	↓ (90%)	A/A	↓ (76%)
A2780- Talc	C/C		C/C		G/G		C/C		A/A	
SKOV-3- Control	C/C	↓ (61%)	C/C	↑ (128%)	G/G	↓ (65%)	C/T	↓ (86%)	A/A	↓ (73%)
SKOV-3- Talc	C/C		T/T		G/G		C/C		A/A	
TOV112D- Control	C/C	↓ (71%)	C/C	↑ (145%)	G/G	↓ (64%)	C/T	↓ (15%)	A/A	↓ (81%)
TOV112D- Talc	C/T		C/C		G/G		C/C		A/A	
HOSEpiC - Control	C/C	↓ (63%)	C/C	↑ (315%)	G/G	↓ (65%)	C/T	↓ (83%)	A/A	↓ (75%)
HOSEpiC-Talc	C/T		T/T		G/G		C/T		A/A	
FT33- Control	C/C	↓ (65%)	C/C	↑ (441%)	G/G	↓ (81%)	C/T	↓ (80%)	A/A	↓ (85%)
FT33-Talc	C/T		T/T		G/G		C/C		A/A	
Normal Ovarian- Control	C/C	↓ (64%)	C/C	↑ (272%)	G/G	↓ (56%)	C/T	↓ (71%)	A/A	↓ (73%)
Normal Ovarian- Talc	C/T		T/T		G/G		C/C		A/A	

Table 2. SNP characteristics (A) and SNP genotyping of key redox enzymes in untreated and talc treated (100 µg/mL) human primary ovarian epithelial cells (Normal ovarian), Human Ovarian Surface Epithelial Cells (HOSEpiC) , fallopian tube (FT33), and ovarian cancer (A2780, SKOV-3, TOV112D) cell lines (B).

259x146mm (300 x 300 DPI)

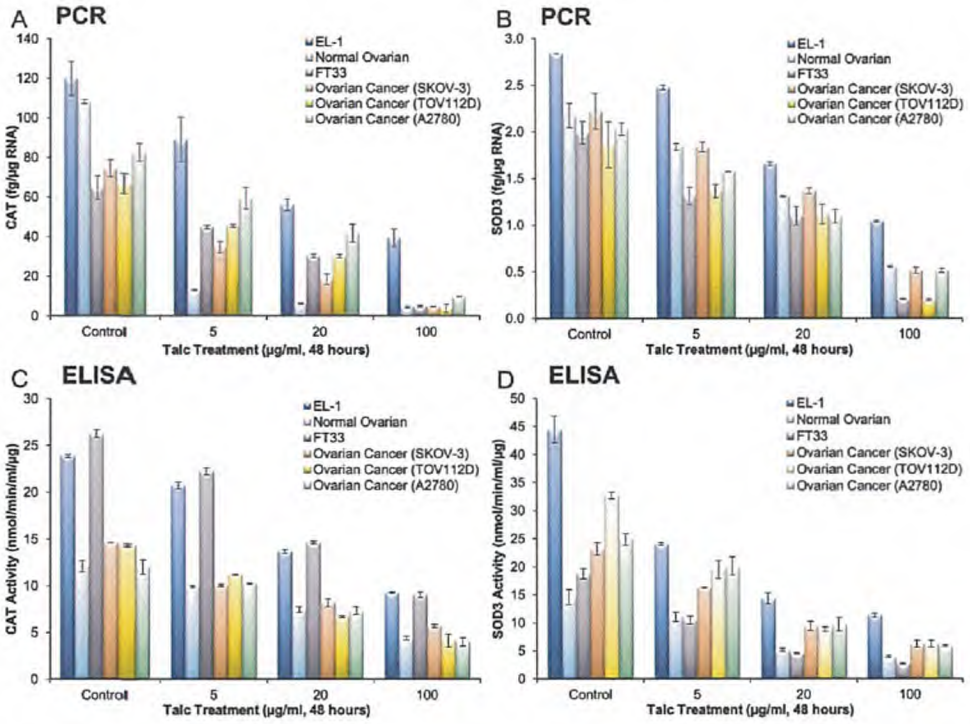

Figure 1. Decreased expression and activity of key antioxidant enzymes, CAT and SOD3. The mRNA (real-time RT-PCR) and protein/activity levels (ELISA) of CAT (A&C) and SOD3 (B&D) were determined in macrophages (EL-1), human primary ovarian epithelial cells (Normal ovarian), fallopian tube (FT33), and ovarian cancer (SKOV-3, TOV112D, and A2780) cell lines before and after treatment with various doses of talc over 48 hours. Experiments were performed in triplicate. Expression is depicted as the mean with error bars representing standard deviation. All changes in response to talc treatment were significant ($p<0.05$) in all cells and in all doses as compared to controls.

254x190mm (300 x 300 DPI)

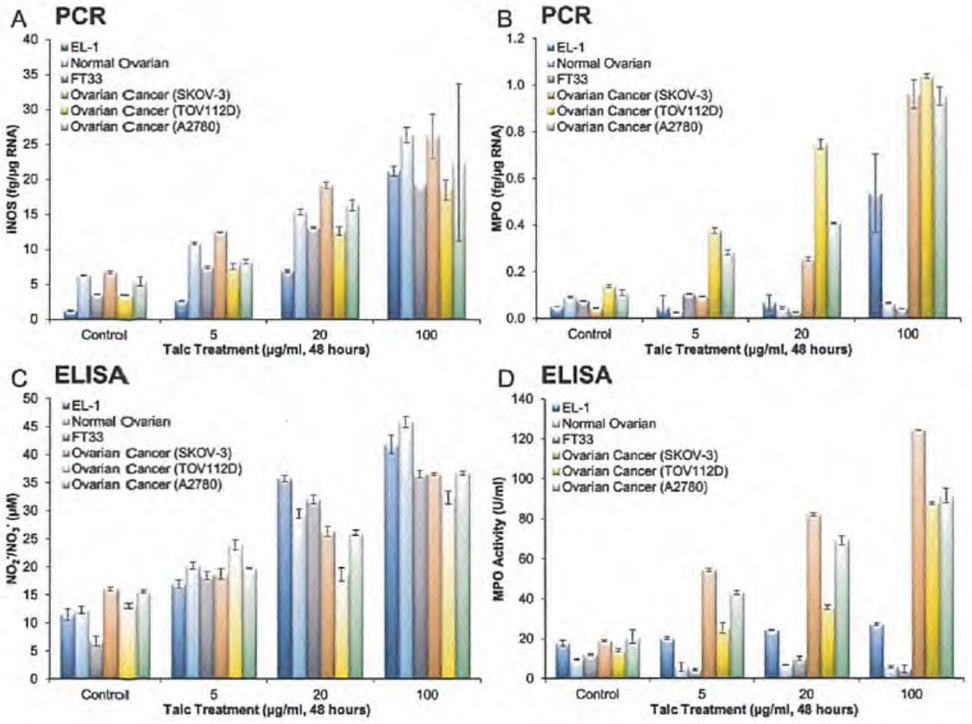

Figure 2. Increased expression and activity of key pro-oxidants, iNOS, NO2-/NO3-, and MPO. The mRNA (real-time RT-PCR) and protein/activity levels (ELISA) of iNOS (A&C) and MPO (B&D) were determined in macrophages (EL-1), human primary ovarian epithelial cells (Normal ovarian), fallopian tube (FT33), and ovarian cancer (SKOV-3, TOV112D, and A2780) cell lines before and after treatment with various doses of talc over 48 hours. As expected, there was no detectable MPO in normal ovarian and fallopian tube cells, and thus talc treatment did not have any effect. Experiments were performed in triplicate. Expression is depicted as the mean with error bars representing standard deviation. All changes in response to talc treatment were significant ($p<0.05$) in iNOS and MPO positive cells and in all doses as compared to controls.

254x190mm (300 x 300 DPI)

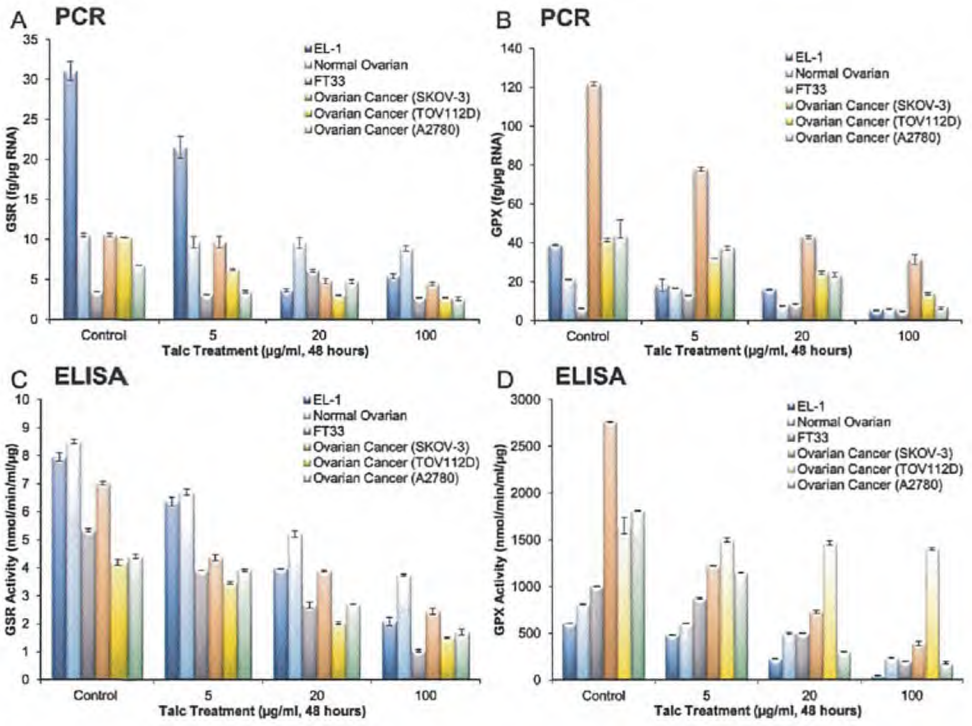

Figure 3. Decreased expression and activity of key antioxidant enzymes, GSR and GPX. The mRNA (real-time RT-PCR) and protein/activity levels (ELISA) of GSR (A&C) and GPX (B&D) were determined in macrophages (EL-1), human primary ovarian epithelial cells (Normal ovarian), fallopian tube (FT33), and ovarian cancer (SKOV-3, TOV112D, and A2780) cell lines before and after treatment with various doses of talc over 48 hours. Experiments were performed in triplicate. Expression is depicted as the mean with error bars representing standard deviation. All changes in response to talc treatment were significant ($p<0.05$) in all cells and in all doses as compared to controls.

254x190mm (300 x 300 DPI)

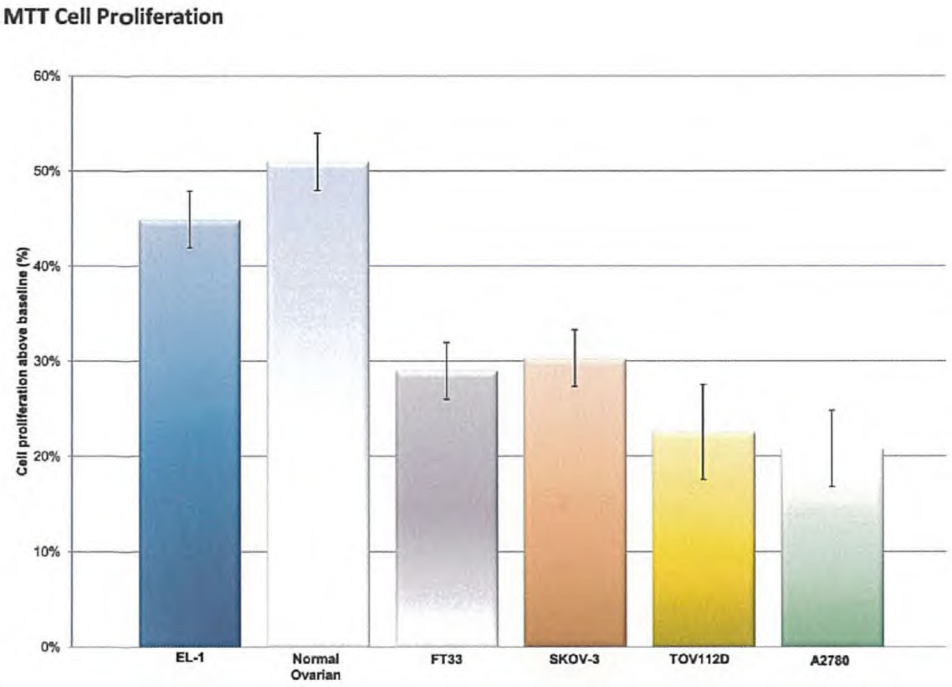

Figure 5. Increased cell proliferation in response to talc treatment. Cell proliferation was determined by MTT Cell Proliferation Assay after 72 hours of talc treatment (100 µg/ml) in macrophages (EL-1), human primary ovarian epithelial cells (Normal ovarian), fallopian tube (FT33), and ovarian cancer (SKOV-3, TOV112D, and A2780) cells. Experiments were performed in triplicate. Cell proliferation is depicted as the mean with error bars representing standard deviation. All changes in response to talc treatment were significant ($p<0.05$) in all cells as compared to controls.

254x190mm (300 x 300 DPI)

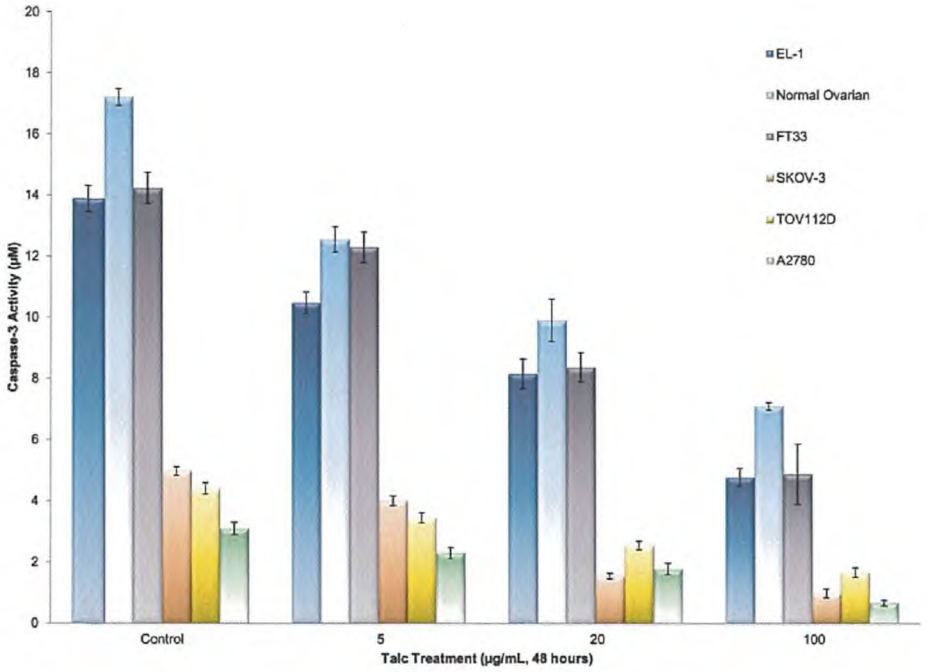

Figure 6. Decreased apoptosis in response to talc treatment. Caspase-3 activity was used to measure the degree of apoptosis in all cells. Caspase-3 Activity Assay was utilized to determine caspase-3 activity in macrophages (EL-1), human primary ovarian epithelial cells (Normal ovarian), fallopian tube (FT33), and ovarian cancer (SKOV-3, TOV112D, and A2780) cell lines before and after treatment with various doses of talc over 72 hours. Experiments were performed in triplicate. Expression is depicted as the mean with error bars representing standard error. All changes in response to talc treatment were significant ($p<0.05$) in all cells and in all doses as compared to controls.

254x190mm (300 x 300 DPI)

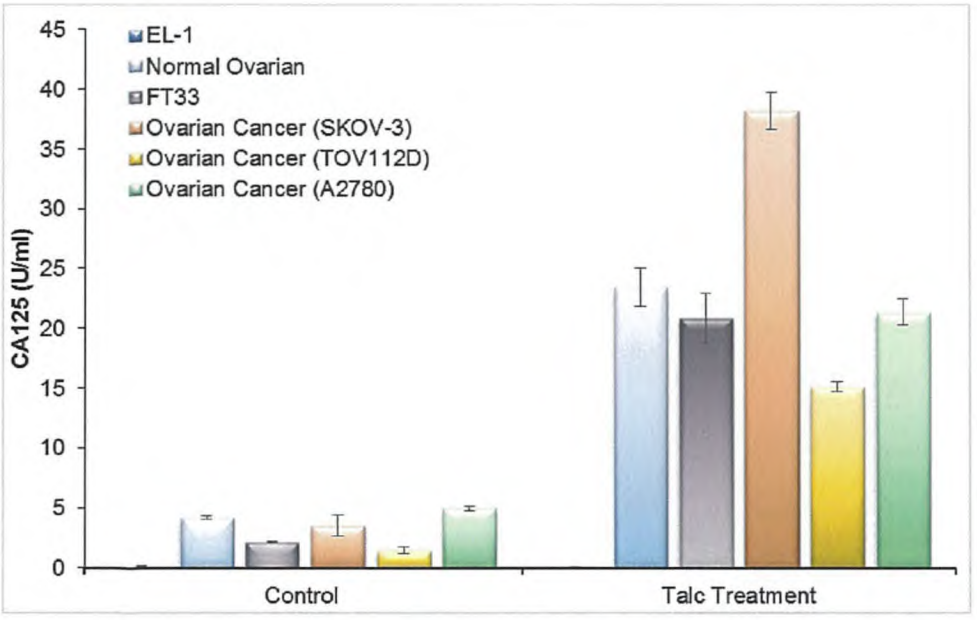

Figure 4. Increased CA125 levels in response to talc treatment. The level of ovarian cancer biomarker CA-125 was determined by ELISA before and after 72 hours of talc treatment (100 µg/ml) in macrophages (EL-1), human primary ovarian epithelial cells (Normal ovarian), fallopian tube (FT33), and ovarian cancer (SKOV-3, TOV112D, and A2780) cells. Experiments were performed in triplicate. Expression is depicted as the mean with error bars representing standard deviation. All changes in response to talc treatment were significant ($p<0.05$) in all cells as compared to controls.

74x47mm (300 x 300 DPI)

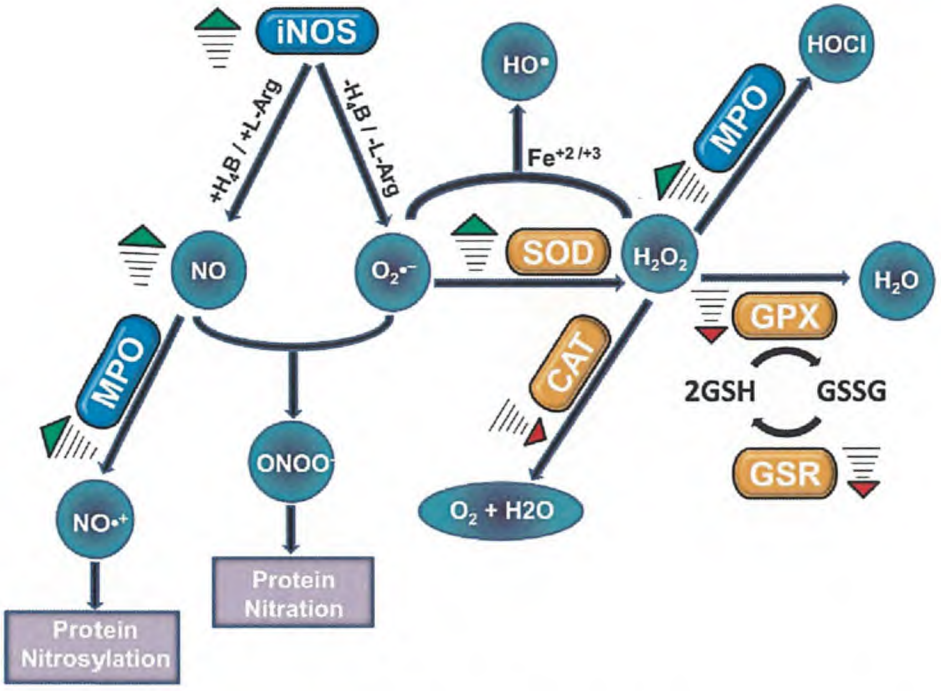

Figure 7. Epithelial ovarian cancer (EOC) cells have been reported to manifest a persistent pro-oxidant state as evident by the upregulation (green arrows) of key oxidants iNOS, NO, NO+, ONOO-, OH-, O2+, and MPO (blue) and downregulation (red arrows) of key antioxidants SOD, CAT, GPX, and GSR (orange). This redox state was also shown to be further enhanced in chemoresistant EOC cells. In this study, talcum powder altered the redox state, as indicated by the arrows, of both normal and EOC cells to create an enhanced pro-oxidant state.

254x190mm (300 x 300 DPI)

Exhibit O

Society for Reproductive Investigation

66th Annual Scientific Meeting

March 12 - 16, 2019 · Palais des Congrès de Paris PARIS, FRANCE

— From Innovation to Impact —

Society for Reproductive Investigation
SRI 2019

Abstract Fee Receipt
Your payment has been received.
Please save this receipt for your records.
Thank you for your submission.

Current Date: 10/11/2018
Name: Harper, Amy
Submission Type: Abstract
Control/Invoice #: 2019-A-1929-SRI
Title: Talcum Powder Enhances Key Mechanisms of Ovarian Cancer Development and Progression: a Link to Increased Ovarian Cancer Risk.

Billing Information:
Ghassan Saed
275 E. Hancock St. Room 243
Detroit, MI 48201
Payment Posted On: 10/11/2018 11:03:40 AM
Payment Type: Visa #### #### #### 1256
Amount Due: $50.00
Amount Paid: $50.00
Amount Billed: $50.00
Balance Due: $0.00

Society for Reproductive Investigation
555 East Wells Street, Suite 1100
Milwaukee, WI 53202-3823
(414) 918-9888

Technical Support
Monday through Friday 8:00AM - 5:00PM Central Standard Time
Phone: 217-398-1792
Email: sri@support.ctimeetingtech.com

Leave cOASIS Feedback

Exhibit P

2019 Annual Meeting Abstract Notification

sgo@confex.com

Thu 11/15/2018 10:38 AM

Inbox

To:Amy Harper <aharper4@med.wayne.edu>;

Dear Amy Harper,

***Please disregard this email if you have already received and accepted the invite through your Speaker Center"**

Congratulations! The Society of Gynecologic Oncology (SGO); SGO President Carol Brown, MD; and 2019 Annual Meeting Program Co-Chairs Wendy Brewster MD, PhD, Diane Yamada MD, are pleased to invite you to present your abstract as a poster at the SGO 50th Annual Meeting on Women's Cancer®, March 16-19, 2019, in Honolulu, Hawaii.

Abstract id: 12691

Abstract Title: Talc induces a pro-oxidant state in normal and ovarian cancer cells through gene point mutations in key redox enzymes

As a poster presenter, you are expected to be at your poster on-site during all dedicated poster viewing times to answer questions and engage learners. As of the time of acceptance, you will be required to be present, but are not required to present your poster orally. The deadline to accept or decline this invitation is, **November 20, 2019 by 11:59 pm CT US.** Failure to respond by this deadline date may result in your abstract being withdrawn. After your acceptance of our invitation, you will receive notifications as your Speaker's Center is updated with the above pertinent poster and logistical information; **all of the information you will need as you prepare for your poster session will be housed in your Speaker's Center and will accessible at your convenience.** Please note: the "General Info" tab that you will see upon logging into your Speaker's Center includes details on all presentation roles of the meeting to keep you informed of the various types of education that will be offered, not just your own role. All forms you complete, however, will be specific to your role(s).

There will be additional activities in this session which you will be receiving correspondence regarding in the coming weeks.

LINK TO SPEAKER'S Center:

https://sgo.confex.com/sgo/2019/speakercenter.cgi?username=17803&password=408314

If the above URL does not work, you may go to:
http://sgo.confex.com/sgo/2019/speakercenter.cgi?

and enter the following:

Username: 17803
Password: 408314

Should you have any issues accessing your Speaker's Center, please do not hesitate to contact Confex Support at (401) 334-0220 or via email at sgo@confex.com. For questions related to Annual Meeting programming, please contact the SGO Education department at education@sgo.org.

Registration & Housing

The Annual Meeting registration fee and housing arrangements are the responsibility of the presenting author, discussant, or moderator. Please visit the Annual Meeting website for additional information on registration and housing.

We look forward to seeing you in Honolulu, Hawaii, at the SGO 50th Annual Meeting, March 16-19, 2019!

Sincerely,

SGO 2019 Annual Meeting Program Committee

Exhibit Q

Begin forwarded message:

From: Reproductive Sciences <onbehalfof@manuscriptcentral.com>
Date: December 26, 2018 at 10:19:59 AM EST
To: gsaed@med.wayne.edu
Cc: lalayman@augusta.edu
Subject: Reproductive Sciences - Decision on Manuscript ID RSCI-18-671
Reply-To: lalayman@augusta.edu

26-Dec-2018

Dear Dr. Saed:Manuscript ID RSCI-18-671 entitled "Molecular basis supporting the association of talcum powder use with increased risk of ovarian cancer" which you submitted to the Reproductive Sciences, has been reviewed. The comments of the reviewer(s) are included at the bottom of this letter.

The reviewer(s) have recommended publication, but also suggest some minor revisions to your manuscript. Therefore, I invite you to respond to the reviewer(s)' comments and revise your manuscript.

To revise your manuscript, log into https://mc.manuscriptcentral.com/rsci and enter your Author Center, where you will find your manuscript title listed under "Manuscripts with Decisions." Under "Actions," click on "Create a Revision." Your manuscript number has been appended to denote a revision.

You will be unable to make your revisions on the originally submitted version of the manuscript. Instead, revise your manuscript using a word processing program and save it on your computer. Please also highlight the changes to your manuscript within the document by using the track changes mode in MS Word or by using bold or colored text.

Once the revised manuscript is prepared, you can upload it and submit it through your Author Center.

When submitting your revised manuscript, you will be able to respond to the comments made by the reviewer(s) in the space provided. You can use this space to document any changes you make to the original manuscript. In order to expedite the processing of the revised manuscript, please be as specific as possible in your response to the reviewer(s).

IMPORTANT: Your original files are available to you when you upload your revised manuscript. Please delete any redundant files before completing the submission.

Because we are trying to facilitate timely publication of manuscripts submitted to the Reproductive Sciences, your revised manuscript should be uploaded as soon as possible. If it is not possible for you to submit your revision in a reasonable amount of time, we may have to consider your paper as a new submission.

Once again, thank you for submitting your manuscript to the Reproductive Sciences and I look forward to receiving your revision.

Sincerely,
Dr. Lawrence Layman
Editor, Reproductive Sciences
lalayman@augusta.edu

Reviewer(s)' Comments to Author:

Reviewer: 1

Comments to the Author
Title: Molecular basis supporting the association of talcum powder use with increased risk of ovarian cancer.

The authors report on the effects of talc in the development of the epithelial ovarian cancer by conducting an in vitro experiment exposing EOC cells to a diluted talc solution. They conclude that the mechanism by which talc alters the cellular redox and inflammatory balance involves the induction of specific mutations in key oxidant and antioxidant enzymes that correlate with alterations in their activities and they claim a genetic predisposition of the EOC cells.

Comments and suggestions:
What is the mechanism by which the ovary and not the vagina, the cervix or the endometrium are susceptibles to talc effects?
What do the authors believe is the determining factor for the increased sensitivity of the epithelial ovarian cells to talc?
The manuscript is "wordy" and would benefit from an attentive reduction.

Exhibit R

Alterations in Gene Expression in Human Mesothelial Cells Correlate with Mineral Pathogenicity

Arti Shukla[1]*, Maximilian B. MacPherson[1]*, Jedd Hillegass[1], Maria E. Ramos-Nino[1], Vlada Alexeeva[1], Pamela M. Vacek[2], Jeffrey P. Bond[3], Harvey I. Pass[4], Chad Steele[5], and Brooke T. Mossman[1]

Departments of [1]Pathology, [2]Medical Biostatistics, and [3]Microbiology and Molecular Genetics, University of Vermont College of Medicine, Burlington, Vermont; [4]Department of Cardiothoracic Surgery, NYU Langone Medical Center, New York, New York; and [5]Department of Medicine, University of Alabama at Birmingham School of Medicine, Birmingham, Alabama

Human mesothelial cells (LP9/TERT-1) were exposed to low and high (15 and 75 $\mu m^2/cm^2$ dish) equal surface area concentrations of crocidolite asbestos, nonfibrous talc, fine titanium dioxide (TiO_2), or glass beads for 8 or 24 hours. RNA was then isolated for Affymetrix microarrays, GeneSifter analysis and QRT-PCR. Gene changes by asbestos were concentration- and time-dependent. At low nontoxic concentrations, asbestos caused significant changes in mRNA expression of 29 genes at 8 hours and of 205 genes at 24 hours, whereas changes in mRNA levels of 236 genes occurred in cells exposed to high concentrations of asbestos for 8 hours. Human primary pleural mesothelial cells also showed the same patterns of increased gene expression by asbestos. Nonfibrous talc at low concentrations in LP9/TERT-1 mesothelial cells caused increased expression of 1 gene Activating Transcription Factor 3 (*ATF3*) at 8 hours and no changes at 24 hours, whereas expression levels of 30 genes were elevated at 8 hours at high talc concentrations. Fine TiO_2 or glass beads caused no changes in gene expression. In human ovarian epithelial (IOSE) cells, asbestos at high concentrations elevated expression of two genes (*NR4A2, MIP2*) at 8 hours and 16 genes at 24 hours that were distinct from those elevated in mesothelial cells. Since *ATF3* was the most highly expressed gene by asbestos, its functional importance in cytokine production by LP9/TERT-1 cells was assessed using siRNA approaches. Results reveal that *ATF3* modulates production of inflammatory cytokines (IL-1β, IL-13, G-CSF) and growth factors (VEGF and PDGF-BB) in human mesothelial cells.

Keywords: mesothelioma; crocidolite asbestos; talc; titanium dioxide; gene profiling

A myriad of natural and synthetic fibers and particles, including nanomaterials, are being introduced into the workplace and environment, and *in vitro* screening tests on human cell types are needed to predict their toxicity and mechanisms of action, especially in target cells of disease. Asbestos is a group of well-characterized fibrous minerals that are associated with the development of nonmalignant (asbestosis) and malignant (lung cancers, pleural, and peritoneal mesotheliomas) diseases in occupational cohorts (1–3), yet the molecular mechanisms of asbestos-related diseases are poorly understood. Although it is widely acknowledged that fibrous geometry, surface and chemical composition, and durability are important features in the development of asbestos-associated diseases, how these contribute to cell toxicity and transformation are unclear. Moreover, the early molecular events leading to injury by asbestos fibers and other pathogenic or innocuous particulates in human cells that may be targets for the development of disease remain enigmatic.

CLINICAL RELEVANCE

Results of work here suggest that transcriptional profiling can be used to reveal molecular events by mineral dusts that are predictive of their pathogenicity in mesothelioma.

The objective of work here was to compare acute toxicity and gene expression profiles of crocidolite asbestos, the type of asbestos most pathogenic in the causation of human mesothelioma (3, 4), to nonfibrous talc, fine titanium dioxide (TiO_2), and glass beads in a contact-inhibited, hTERT-immortalized human mesothelial cell line (5). In comparative studies, we also evaluated toxicity of particulates and gene expression changes in a contact-inhibited SV40 Tag-immortalized human ovarian epithelial cell line (IOSE) (6). This cell type is not implicated in asbestos-induced diseases, but is occasionally linked to inflammation and the development of ovarian cancer after use of talcum powder in the pelvic region, although such links are highly controversial (7).

Although most studies have evaluated the biological effects of particles and fibers on an equal mass or weight basis, the number, surface area, and reactivity of particulates at equal weight concentrations may be vastly different. Moreover, recent *in vitro* (8, 9) and *in vivo* (10–12), studies have confirmed that toxicity, oxidative stress, and inflammatory effects of ultrafine and other particles are related directly to surface area. For these reasons, and to avoid possible confounding alterations in gene expression or toxicity that might reflect or be masked in cells in different phases of the cell cycle, we introduced particulates at equal surface areas to confluent monolayers of human mesothelial (LP9/TERT-1) and human ovarian epithelial (IOSE) cells in a maintenance medium. Moreover, our studies included a nonfibrous talc sample and fine TiO_2 and glass particles, both traditionally used as nontoxic and nonpathogenic control particles in *in vitro* and animal experiments (reviewed in Refs. 13 and 14). Our studies provide novel insight into the early molecular events and responses occurring in human cells after exposure to asbestos and these materials.

MATERIALS AND METHODS

Human Mesothelial and Ovarian Epithelial Cell Cultures

Human mesothelial LP9/TERT-1 (LP9) cells, an hTERT-immortalized cell line phenotypically and functionally resembling normal human mesothelial cells (5), were obtained from Dr. James Rheinwald (Dana Farber Cancer Research Institute, Boston, MA). Human pleural mesothelial cells (NYU474) were isolated surgically from

(*Received in original form April 11, 2008 and in final form November 24, 2008*)

* These authors contributed equally to this research.

This work was supported by NIEHS training grant T32ES007122 to B.T.M., a contract from EUROTALC and the Industrial Minerals Association of North America, and NCI P01 CA 114,047 (H.I.P. and B.T.M.).

Correspondence and requests for reprints should be addressed to Arti Shukla, Ph.D., Department of Pathology, University of Vermont College of Medicine, 89 Beaumont Avenue, Burlington, VT 05405. E-mail: Arti.Shukla@uvm.edu

This article contains microarray data which can be found as a repository using the accession number GSE14034.

Am J Respir Cell Mol Biol Vol 41. pp 114–123, 2009
Originally Published in Press as DOI: 10.1165/rcmb.2008-0146OC on December 18, 2008
Internet address: www.atsjournals.org

cancer-free patients by Dr. Harvey Pass (New York University, New York, NY). Briefly, tissue sample 2 × 2 cm^2 was harvested into saline solution and rinsed immediately with PBS (1×) and Dulbecco's modified Eagle's medium (DMEM) (1×). The tissue was then digested with 0.2% Collagenase type 1 (MP Biomedical Inc., Solon, OH) for 3 hours at 37°C. Finally, the digested tissue was scraped and cells collected were centrifuged for 5 minutes at 300 × *g*. The cell pellet thus obtained was resuspended in DMEM containing 10% fetal bovine serum (FBS) and 2% penicillin–streptomycin, transferred into 6-well plate, and allowed to grow at 5% CO_2 and 37°C. Mesothelial cells were characterized by staining with calretinin antibody. An SV40 Tag-immortalized, anchorage-dependent human ovarian epithelial cell line (IOSE 398) (6) was a kind gift from Dr. Nelly Auersperg (Canadian Ovarian Tissue Bank, University of British Columbia, Vancouver, BC, Canada). LP9/TERT-1 cells were maintained in 50:50 DMEM/F-12 medium containing 10% FBS, and supplemented with penicillin (50 units/ml), streptomycin (100 μg/ml), hydrocortisone (100 μg/ml), insulin (2.5 μg/ml), transferrin (2.5 μg/ml), and selenium (2.5 μg/ml). IOSE cells were maintained in 50:50 199/MCB105 medium containing 10% FBS and 50 μg/ml gentamicin. Cells at near confluence were switched to maintenance medium containing 0.5% FBS for 24 hours before particulate exposure. NYU474 cells were grown to near confluence in DMEM containing 10% FBS and supplemented with penicillin (50 units/ml) and streptomycin (100 μg/ml).

Characterization of Mineral Preparations

The physical and chemical characterization of the NIEHS reference sample of crocidolite asbestos has been reported previously (15). The surface area of asbestos fibers and particles was measured using nitrogen gas sorption analysis to allow computation of identical amounts of surface areas of particulates to be added to cells. Fiber and particle size dimensions were determined by scanning electron microscopy (SEM) as described previously (16). In addition, talc was examined using field emission scanning electron microscopy (FESEM) and transmission electron microscopy (TEM). The chemical composition, surface area, mean size, and source of each particulate preparation is presented in Table 1.

Introduction of Particulates to Cells

After sterilization under ultraviolet light overnight to avoid endotoxin and microbial contamination, particulates were suspended in HBSS at 1 mg/ml, sonicated for 15 minutes in a water bath sonicator, and triturated five times through a 22-gauge needle. This suspension was added to cells in medium.

SEM to Determine Particulate/Cell Interactions

Cells were grown on Thermonox plastic cover slips (Nalge Nunc International, Naperville, IL), exposed to particulates for 24 hours, and then processed for SEM as described previously (16). After samples were critical point-dried, they were mounted on aluminum specimen stubs and dried before being sputter-coated with gold and palladium in a Polaron sputter coater (Model 5100; Quorum Technologies, Guelph, ON, Canada) and examined on a JSM 6060 scanning electron microscope (JEOL USA, Inc., Peabody, MA).

Cell Viability Studies

After 24 hours, cells were collected with Accutase cell detachment reagent, and final cell suspensions in Accutase/complete medium/HBSS were mixed with 0.4% trypan blue stain, which is retained by dead cells. After 5 minutes, unstained cells were counted using a hemocytometer to determine the total number of viable cells per dish.

Based on the results of cell viability studies, asbestos and nonfibrous talc were evaluated in LP9 mesothelial cells for changes in gene expression at both low and high concentrations (15 and 75 $\mu m^2/cm^2$ dish) at 8 hours, and at low concentrations of minerals (15 $\mu m^2/cm^2$ dish) at 24 hours. These concentrations did not cause morphologic or toxic cellular changes at these time points. Negative control groups included cells exposed to fine TiO_2 (15 $\mu m^2/cm^2$ dish) at 8 and 24 hours and glass beads (75 $\mu m^2/cm^2$) at 24 hours. In IOSE cells, gene expression of all particulates was evaluated at 75 $\mu m^2/cm^2$ at 8 and 24 hours, as preliminary experiments revealed that no significant changes in mRNA levels were observed at 15 $\mu m^2/cm^2$ dish of asbestos. In NYU474 human mesothelial cells, QRT-PCR was used to validate a selected subset of gene expression changes identified by arrays in LP9/TERT-1 cells. Cells were exposed to 15 and 75 $\mu m^2/cm^2$ asbestos for 24 hours, and 8 genes highly expressed in LP9 cells were examined by QRT-PCR (*see below*).

RNA Preparation

Total RNA was prepared using an RNeasy Plus Mini Kit according to the manufacturers' protocol (Qiagen, Valencia, CA), as previously described (17).

Affymetrix Gene Profiling

Microarrays were performed on samples from three independent experiments. All cell types, time points, and mineral types and concenrations were included in all three experiments. For each experiment, $n = 3$ dishes were pooled into one sample per treatment group. Each of the pooled samples was analyzed on a separate array (i.e., $n = 3$ arrays per condition [3 independent biological replicates]). All procedures were performed by the Vermont Cancer Center DNA facility using standard Affymetrix protocol as previously described (14, 17). Each probe array, Human U133A 2.0 (Affymetrix, Santa Clara, CA) was scanned twice (Hewlett-Packard GeneArray Scanner, Palo Alto, CA), the images overlaid, and the average intensities of each probe cell compiled. Microarray data were analyzed using GeneSifter software (VizX Labs, Seattle, WA). This program used a "*t* test" for pairwise comparison and a Benjamini-Hochberg test for false discovery rate (FDR 5%) to adjust for multiple comparisons. A 2-fold cutoff limit was used for analysis.

Quantitative Real-Time PCR

Total RNA (1 μg) was reverse-transcribed with random primers using the Promega AMV Reverse Transcriptase kit (Promega, Madison, WI) according to the recommendations of the manufacturer, as described previously (17). In NYU474 mesothelial cells, eight genes (*ATF3*, *SOD2*, *PTGS2*, *FOSB*, *TFPI2*, *PDK4*, *NR4A2*, and *IL-8*) most highly expressed in LP9 cells were evaluated using the ΔΔCt method. Duplicate or triplicate assays were performed with RNA samples isolated from at least three independent experiments. The values obtained from cDNAs and hypoxanthine phosphoribosyl transferase (*hprt*) controls provided relative gene expression levels for the gene locus investigated. The primers and probes used to validate gene expression as observed in microarrays were purchased from Applied Biosystems (Foster City, CA).

TABLE 1. CHARACTERIZATION OF PARTICULATES

Name	Chemical Composition	Mean Surface Area ± SE (m^2/g)	Mean Size (μm)*	Source
Crocidolite Asbestos	$Na_2Fe_3^{2+}Fe_2^{3+}Si_8O_{22}(OH)_2$	14.97 ± 0.605	7.4 × 0.25	NIEHS Reference Sample
Talc (MP 10-52)†	$Mg_3Si_4O_{10}(OH)_2$	16.03 ± 0.654	1.1	Barrett's Minerals, Inc.
Titanium Dioxide	TiO_2	9.02 ± 0.185	0.69	Fisher Scientific
Glass Beads	SiO_2	2.78 ± 0.215	2.06	Polysciences Inc.

* Length X width for crocidolite asbestos, and diameter for nonfibrous talc, TiO_2, and glass beads.

† Although standard reference samples of asbestos and some particulates are available for use by the scientific community, reference samples of talc currently do not exist. For these reasons, the nonfibrous talc sample was also characterized for physical properties, particle size distribution (0.70 μm minimum to 1.20 μm maximum), and chemical/mineralogical (talc 95%, chlorite 4.5–5%, dolomite 0.3%) composition. For complete analysis or obtaining samples, please contact Brooke Mossman, Mark Ellis (markellis@ima-na.org), or Michelle Wyart at EUROTALC (mwyart@ima-europe.eu).

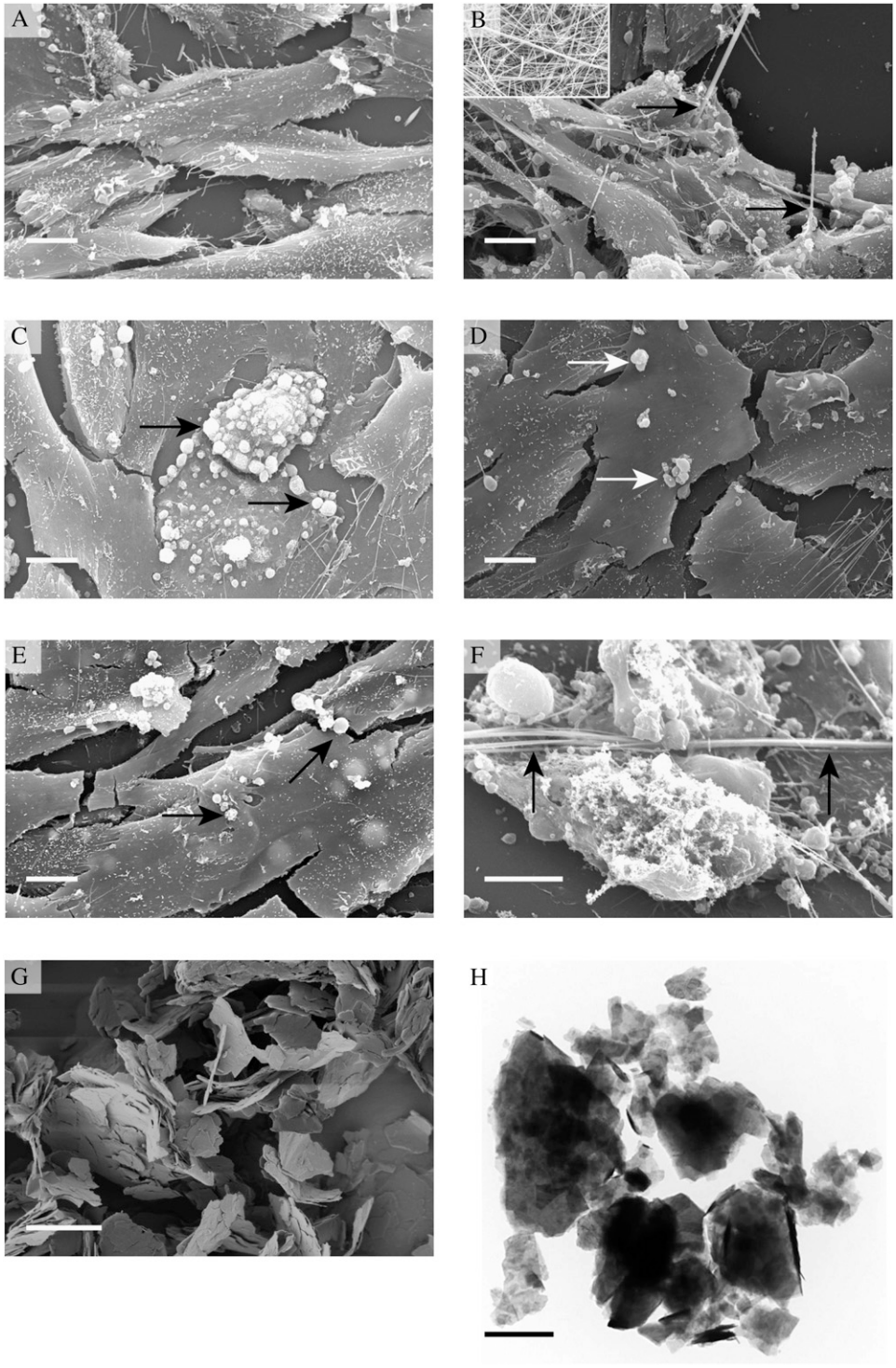

Figure 1. Interaction of fibers and particles with (*A–E*) LP9/TERT-1 human mesothelial cells and (*F*) IOSE ovarian epithelial cells after 24 hours of exposure to (*B, E, F*) high and (*C, D*) low concentrations of particulates. (*G*) Field emission scanning electron microscopy (FESEM) and (*H*) transmission electron microscopy (TEM) show structure of nonfibrous talc. (*A*) Morphology of unexposed near-confluent LP9/TERT-1 cells. (*B*) Membrane blebbing and piling up of cells in response to crocidolite asbestos (*arrows*). (*C*) Nonfibrous talc and (*D*) fine TiO_2 (*arrows*) on cell surface. (*E*) Single and small clumps of glass beads on plasma membrane. (*F*) Interaction of asbestos fibers (*arrows*) with IOSE cells that exhibit an exudate and membrane ruffling in response to fibers. *Bars* = 10 μm. (*G*) FESEM and (*H*) TEM showing morphology of platy talc bulk material. *Bars* = 2 μm.

Transfection of LP9 Cells with siRNA

On-Target plus Non-targeting siRNA #1 (scrambled control), and On-Target plus SMART pool human *ATF3* siRNA (100 nM; Dharmacon, Lafayette, CO) were transfected into LP9 cells at near confluence using Lipofectamine 2000 (Invitrogen, Carlsbad, CA), following the manufacturer's protocol. The efficiency of *ATF3* knockdown was determined by QRT-PCR after 48 and 72 hours.

Bio-Plex Analysis of Cytokine and Chemokine Concentrations in Medium of LP9/TERT-1 Cells

To quantify cytokine and chemokine levels in conditioned medium of cells transfected with siATF3 or scrambled control and exposed to asbestos for 24 hours, a multiplex suspension protein array was performed using the Bio-Plex protein array system as described previously (17) and a Human Cytokine 27-plex panel (Bio-Rad, Hercules, CA). Three biological replicates were used for each treatment group.

Statistical Analysis

Data from QRT-PCR and cell viability assays were evaluated by ANOVA using the Student Neuman-Keul's procedure for adjustment of multiple pairwise comparisons between treatment groups or using the nonparametric Kruskal-Wallis and Mann-Whitney tests. Differences with P values ≤ 0.05 were considered statistically significant.

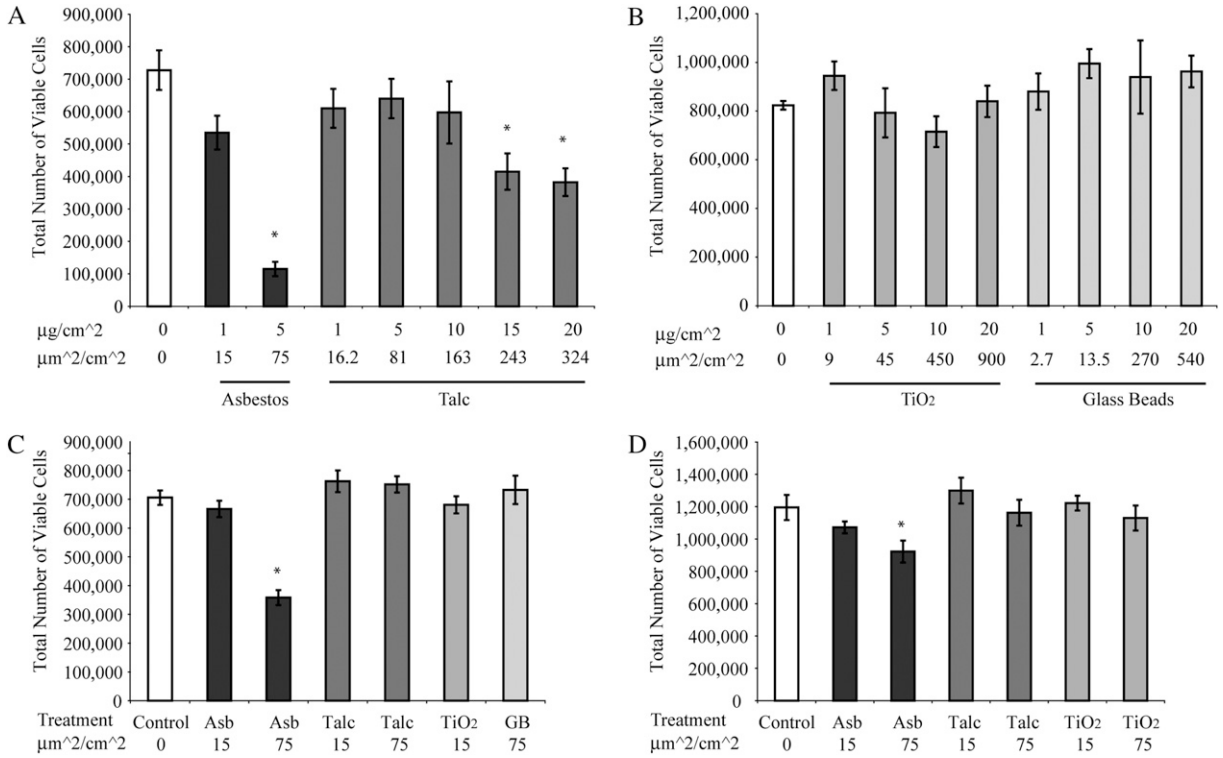

Figure 2. Cell viability after 24 hours of exposure to asbestos fibers and particles in (*A–C*) LP-9/TERT-1 and (*D*) IOSE (D). Mean +/− SE of 1 (A, B) or 3 (C, D) individual experiments where $n = 3$ per group per experiment. * $P \leq 0.05$ compared with untreated (0) groups.

RESULTS

Characterization of Particulate Preparations

Table 1 shows the major chemical formulas of crocidolite asbestos fibers (defined as having a greater than 3:1 length to width ratio) and particle samples used in experiments, although trace amounts of other elements occur in the NIEHS asbestos standards (15). In addition, we examined the morphology and cellular interactions of asbestos fibers, talc, and other particles using SEM (Figure 1). These studies revealed that only high (75 $\mu m^2/cm^2$) surface area concentrations of asbestos caused membrane blebbing and other toxic manifestations in cells (Figures 1B and 1F). In contrast, particles of nonfibrous talc (Figure 1C), fine TiO_2 (Figure 1D), and glass beads (Figure 1E) were nontoxic. Both asbestos fibers and particles were observed on the cell surface and were encompassed by cells. Nonfibrous talc occurred in platy particles that were uniform in appearance as viewed by FESEM (Figure 1G) and TEM (Figure 1H).

Asbestos Fibers at High Concentrations Are Toxic to LP9/TERT-1 Human Mesothelial Cells and Less So to Ovarian Epithelial Cells in Contrast to Particle Preparations

Figure 2 shows the results of trypan blue exclusion tests in LP9/TERT-1 and IOSE cells. In LP9/TERT-1 cells (Figures 2A–2C), asbestos at high surface area concentrations (75 $\mu m^2/cm^2$) caused significant decreases (50–80%) in cell viability that were more striking than those observed in IOSE cells (Figure 2D). Nonfibrous talc at 75 $\mu m^2/cm^2$ was nontoxic, and significant increases in toxicity were only achieved with addition of talc at $\geq$ 3-fold higher concentrations in LP9/TERT-1 cells (Figure 2A), but not in IOSE cells (data not shown). Neither TiO_2 nor glass beads were significantly toxic to either cell type over a range of concentrations (Figure 2B).

Asbestos Fibers, but Not Particle Preparations, Cause Dose- and Time-Related Changes in Gene Expression in Human LP9 Mesothelial Cells

Figure 3 shows a summary of significantly increased or decreased (> 2-fold compared with untreated controls) gene expression by asbestos (Figures 3A–3C) and nonfibrous talc (Figure 3D) in LP9/TERT-1 cells as well as the classification of genes by ontology. These studies revealed that gene expression changes by low concentrations of asbestos were less (29 increases) than at high concentrations (236 alterations including decreases) at 8 hours. Moreover, numbers of significant mRNA level alterations (205) at low concentrations of asbestos increased over time. In contrast, fewer numbers (30) of gene expression increases were observed at high concentrations of talc at 8 hours compared with identical surface areas of asbestos (236 changes), and no decreases in gene expression were observed. No significant alterations in gene expression were observed with low concentrations of talc at 24 hours or with TiO_2 or glass beads at either concentration or time point (data not shown). The major genes affected by asbestos or talc in LP9/TERT-1 cells are listed in Tables 2–4. This information reveals that the fold-increases in common genes expressed by asbestos-treated cells increase in a dose-related fashion at 8 hours. Although dose–responses were observed with talc at 8 hours, the numbers of significant gene increases as well as fold-increases were less than that observed with asbestos and decreased over time. Since mRNA expression of *ATF3* and *IL8* were increased by either asbestos or talc in LP9/TERT-1 cells, the increased expression of these genes was verified by QRT-PCR in mineral-exposed cells as compared with untreated control cells (Figure 4).

In NYU474 cells, QRT-PCR was used to validate that eight asbestos-induced genes in LP9 cells were up-regulated in

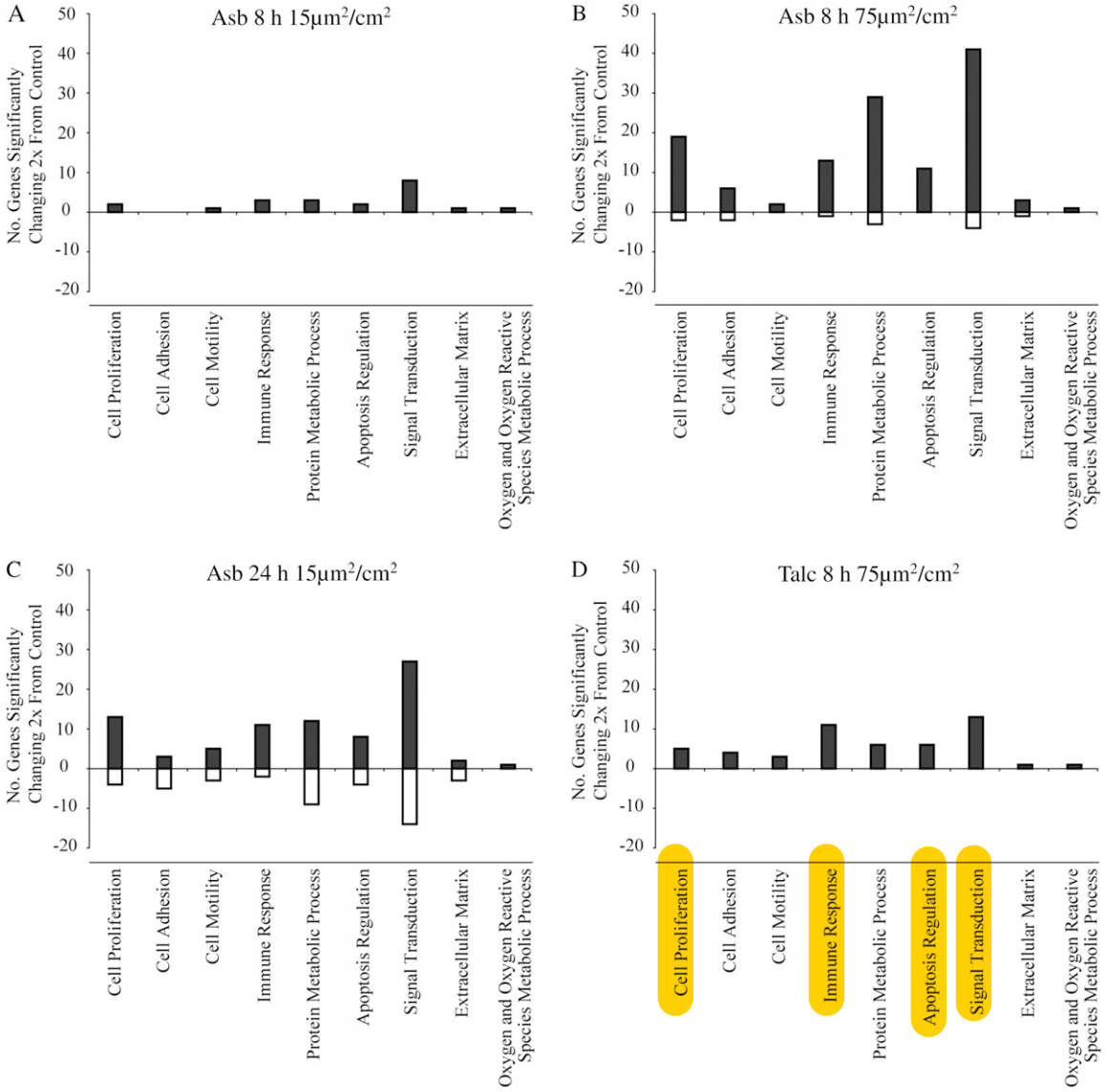

Figure 3. Numbers of changes ($P \leq 0.05$) in gene expression and classification by ontology in LP9/TERT-1 cells after exposure to (*A*–*C*) crocidolite asbestos or (*D*) nonfibrous talc.

normal human mesothelial cells (*ATF3*, *PTGS2* or *COX2*, *FOSB*, *IL8*, *NR4A2*, and *TFPI2*). Results showed that mRNA levels of six of the eight genes evaluated were increased in a dose-responsive fashion after exposure to asbestos for 24 hours (Figure 5).

IOSE Ovarian Epithelial Cells Exhibit Few Gene Expression Changes in Response to Asbestos

In contrast to LP9/TERT-1 and NYU474 mesothelial cells, IOSE cells showed no significant gene up-regulation or down-regulation in response to lower concentrations of asbestos at 8 or 24 hours (data not shown). At high concentrations of asbestos at 8 hours, mRNA levels of only two genes (*NR4A2* and *CXCL2* or *MIP2*) were increased in comparison to untreated IOSE cells (Table 4). At 24 hours, high concentrations of asbestos caused less than 4-fold increases in expression of only 16 genes, and decreased expression of 1 gene, *Profilin 1* (data not shown). No significant mRNA changes were observed with nonfibrous talc, fine TiO_2 or glass beads at either time point.

Inhibition of *ATF3* by siRNA Alters Asbestos-Induced Cytokines in LP9/TERT-1 Cells

Since *ATF3* was a common gene up-regulated by asbestos in mesothelial cells its functional role in cytokine production in LP9 cells was evaluated. As shown in Figure 6A, *ATF3* was successfully inhibited in LP9/TERT-1 cells using siATF3 as described in Materials and Methods. Cells transfected with control siRNA or siATF3 were then exposed to asbestos (75 $\mu m^2/cm^2$ $n = 3$) for 24 hours, and medium was collected and analyzed for cytokines and growth factors using Bio-Plex analyses. Inhibition of *ATF3* altered levels of asbestos-induced inflammatory cytokines (IL-1β, IL-13, G-CSF) and the growth factor (PGDF-BB) in LP9/TERT-1 cells (Figure 6B). Trends in diminishing levels of VEGF were also observed, although not statistically significant.

DISCUSSION

Gene expression analysis has been used for the classification of soluble toxicants in rodent and human cells *in vitro*. Models of

TABLE 2. TOP 10 GENES AFFECTED BY CROCIDOLITE ASBESTOS AT 8 AND 24 H IN LP9/TERT-1 HUMAN MESOTHELIAL CELLS

Concentration	Low (*15* $\mu m^2/cm^2$)		High (*75* $\mu m^2/cm^2$)
Time	8 h	24 h	8 h
	Fold Change		
Up-regulated			
Activating transcription factor 3 (*ATF3*)	9	9	27
Prostaglandin-endoperoxide synthase 2 (PTGS2)	7	8	16
Superoxide Dismutase 2 (SOD2)	6	6	2
Chemokine (C-X-C motif) ligand 3 (CXCL3)	4	NC	16
FBJ murine osteosarcoma viral oncogene homolog B (FOSB)	4	NC	NC
Tissue factor pathway inhibitor 2 (TFPI2)	4	14	11
Pyruvate dehydrogenase kinase, isozyme 4 (PDK4)	3	9	15
Chemokine (C-X-C motif) ligand 2 (CXCL2)	3	NC	NC
Angiopoietin-like 4 (ANGPLT4)	3	NC	NC
Kruppel-like factor 4 (gut) (KLF4)	3	NC	NC
Interleukin 8 C-terminal variant, 211506_s_t (IL8)	NC	8	12
Interleukin 1 receptor-like 1 (IL1R1)	NC	6	11
Nuclear receptor subfamily 4 (NR4A2)	NC	NC	11
Solute carrier family 7 (SLC7A2)	NC	6	10
Pleckstrin homology-like domain (PHLDA1)	NC	7	NC
Interleukin 8 (IL8)	NC	6	NC
Down-regulated			
Inhibitor of DNA binding 3 (ID3)	NC	NC	−5
Inhibitor of DNA binding 1 (ID1)	NC	NC	−3
Cytochrome P450, family 24 (CYP24A1)	NC	NC	−3
Basic helix-loop-helix domain (BHLHB3)	NC	NC	−3
SMAD family member 6 (SMAD6)	NC	NC	−3
S-phase kinase associated protein 2 (SKP2)	NC	NC	−3
Cadherin 10, type 2 (CDH10)	NC	NC	−3
START domain containing 5 (STARD5)	NC	NC	−3
211042_x_at	NC	NC	−2
Interferon-induced protein with tetratricopeptide (IFIT1)	NC	NC	−2
Oxytocin receptor (OXTR)	NC	−6	NC
Transcribed locus	NC	−5	NC
Chromosome 5 open reading frame (C5orf13)	NC	−5	NC
Cytochrome P450, family 24 (CYP24A1)	NC	−4	NC
Chromosome 21 open reading frame (C21orf7)	NC	−3	NC
KIAA1199	NC	−3	NC
Methyltransferase like 7A (METTL7A)	NC	−3	NC
PDZ domain containing RING finger 3 (PDZRN3)	NC	−3	NC
Periplakin (PPL)	NC	−3	NC
Phospholipase-C-like 1 (PLCL1)	NC	−3	NC

Definition of abbreviation: NC, no significant ($P \leq 0.05$) change > 2-fold from control.

transcript profiling for discrimination of toxic and nontoxic compounds in liver and other organs have also been developed in rodents (18), confirming the hypothesis that predictive modeling for classification of toxic agents and carcinogens is feasible. Here we used toxicogenomic approaches in human mesothelial cells, a cell type exquisitely sensitive to asbestos (19) and human contact-inhibited ovarian epithelial cells, a cell type not linked to carcinogenesis by asbestos, to determine whether the magnitude of altered gene expression by insoluble particulates correlated with their toxicity to cells and documented pathogenicity in humans. Although a recent study has examined gene expression profiles comparatively in crocidolite asbestos–exposed human lung adenocarcinoma (A549) and SV40-immortalized bronchial (BEAS-2B) or pleural mesothelial cell lines (MET5A) by cluster analysis (20), our studies are the first to examine gene expression changes by asbestos in comparison to other well-characterized particles in a human cell line that exhibits features of normal mesothelial cells (5). Although strict comparisons between cell types are not justified because SV40 Tag was used to immortalize the IOSE ovarian epithelial cell line (6), and SV40 infection is known to decrease sensitivity of human mesothelial cell lines to toxicity by asbestos (21), our studies suggest that the increased numbers of gene expression alterations observed in LP9/TERT-1 human mesothelial cells reflect elevated sensitivity of this cell type to asbestos. NYU474 human mesothelial cells were more resistant that LP9/TERT-1 cells to asbestos toxicity, permitting us to perform QRT-PCR studies at both concentrations of asbestos at 24 hours. These results confirmed common dose-related patterns of gene expression in mesothelial cells versus ovarian epithelial (IOSE) cells.

It is generally recognized that geometry and length and width (i.e., aspect ratio) of durable fibers such as amphibole asbestos types (crocidolite, amosite) are important properties determining toxicity, transforming potential, and carcinogeniciy in rodents and humans (13, 22, 23). Since talc can occur in various geometries (nonfibrous and fibrous) and can be contaminated with other minerals, including amphiboles, in some mining deposits (reviewed in Ref. 24), we used a well-characterized, nonfibrous talc sample here to allow evaluation of a particle not causing mesotheliomas or pleural sarcomas in rodents (23). Moreover, nonfibrous talc is regarded as noncarcinogenic in humans (25). Since talc is a magnesium silicate, and Mg^{2+} may interact with negatively charged molecules on the cell surface to

TABLE 3. GENES UP-REGULATED BY NONFIBROUS TALC IN LP9/TERT-1 HUMAN MESOTHELIAL CELLS

Gene	Fold Increase
8 h Low (15 $\mu m^2/cm^2$)	
Activating transcription factor 3 (*ATF3*)	3
8 h High (75 $\mu m^2/cm^2$)	
Activating transcription factor 3 (*ATF3*)	13
Inhibin, beta A (INHBA)	9
Chemokine (C-X-C motif) ligand 3 (CXCL3)	7
Superoxide dismutase 2 (SOD2)	7
Interleukin 8 C-terminal variant, 211506_s_t (IL8)	6
Prostaglandin-endoperoxide synthase 2 (PTGS2)	5
Interleukin 8 (IL8)	5
FBJ murine osteosarcoma viral oncogene homolog B (FOSB)	5
Tumor necrosis factor alpha-induced protein 6 (TNFAIP6)	4
Tissue factor pathway inhibitor 2 (TFPI2)	4
Chemokine (C-X-C motif) ligand 2 (CXCL2)	3
Intercellular adhesion molecule 4 (CICAM4)	3
ChaC, cation transport regulator homolog 1 (ChaC 1)	3
Nuclear receptor subfamily 4, group A, member 3 (NR4A3)	3
Pleckstrin homology-like domain, family A, member 1 (PHLDA1)	3
Interleukin 6 (IL-6)	3
Phorbol -12-myristate-13-acetate-induced protein 1 (PMA1P1)	3
Oxidized low density lipoprotein (lectin-like) receptor 1 (OLR1)	3
Chemokine (C-C motif) ligand 20 (CCL20)	3
v-maf musculoaponeurotic fibrosarcoma oncogene homolog F	3
Interleukin 1, alpha (IL-1α)	2
Tumor necrosis factor-α induced protein 3 (TNFA1P3)	2
Interleukin 1 receptor-like 1 (IL1RL1)	2
Angiopoieten-like 4 (ANGPLT4)	2
Kruppel-like factor 4 (KLF4)	2
GTP binding protein overexpressed in skeletal muscle (GEM)	2
Pentraxin-related gene, rapidly induced by IL-1 beta (PTX3)	2
Interleukin 1 beta (IL-1β)	2
HSPB (heat shock 27 kD) associated protein 1 (HSPBAP1)	2
Kynureninase (KYNU)	2

disturb cell homeostasis (reviewed in Ref. 26), this may explain the few mRNA expression increases that were observed initially with talc at 8 hours. However, these changes were not observed at 24 hours, suggesting that human mesothelial cells adapt to or undergo repair after exposure to this mineral.

Our gene profiling data here and in inhalation studies using chrysotile asbestos (14) also support the concept that fine TiO_2 is nontoxic and nonpathogenic to mesothelial or other cell

TABLE 4: GENES UPREGULATED BY CROCIDOLITE ASBESTOS IN IOSE HUMAN OVARIAN CELLS

Gene	Fold increase
8 h High (75 $\mu m^2/cm^2$)	
Nuclear receptor subfamily 4 (NR4A2)	4
Chemokine (C-X-C motif) ligand 2 (MIP2)	2
24 h High (75 $\mu m^2/cm^2$)	
Nuclear receptor subfamily 4 (NR4A2)	4
DNA-damage-inducible transcript 3 (DDIT3)	3
Stromal cell-derived factor 2-like 1(SDF2L1)	3
Heat shock 70 kD protein 1A (HSPA1A)	3
DnaJ (Hsp40) homolog, subfamily C (DNAJC3)	2
Paraspeckle component 1	2
Heat shock 70 kD protein 1B (HSPA1B)	2
Homocysteine-inducible, endoplasmic reticulum stress-inducible, ubiquitin-like domain member (HERPUD1)	2
Serum/glucocorticoid regulated kinase family, member 3 (SKG3)	2
DnaJ (Hsp40) homolog, subfamily B, member 9 (DNAJB9)	2
Arginine-rich, mutated in early stage tumors (ARMET)	2
Syntaxin 1A (brain) (STX1A)	2
Heat shock 70 kD protein 5 (HSPA5)	2
ADAM metallopeptidase with thrombospondin type 1 motif	2
Heat shock protein 90kDa beta (Grp94), member 1 (HSP90B1)	2

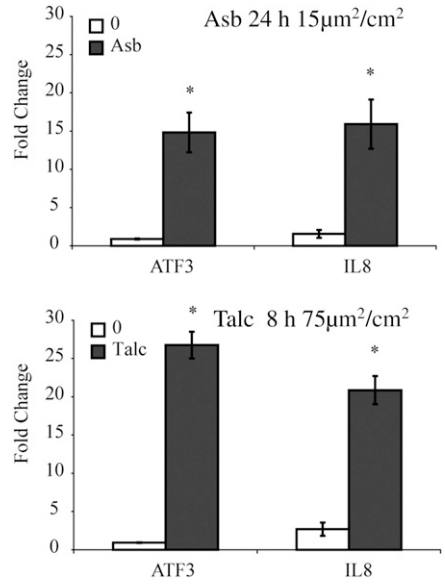

Figure 4. QRT-PCR confirms significant increases in *ATF3* and *IL8* expression by crocidolite asbestos at low concentrations and nonfibrous talc at high concentrations in LP9/TERT-1 mesothelial cells. *$P < 0.05$ as compared to untreated (0) groups.

types. Likewise, in the rat, inhalation of fine TiO_2 (defined as particles > 0.1 μm in diameter), in contrast to ultrafine (particles < 0.1 μm in diameter) does not give rise to predictive markers of toxicity, inflammation, pulmonary fibrosis, or oxidative stress, as indicated by elevated levels of Mn-containing superoxide dismutase (*SOD2*) in cells from bronchopulmonary lavage (27). The increased reactivity and toxicity of ultrafine particles as compared with larger fine or coarse particles have also been confirmed in a number of *in vitro* and *in vivo* experiments and is often attributed to their increased surface area and/or ability to penetrate lung cells.

Our studies reveal a number of novel genes induced by asbestos in LP9/TERT-1 cells. As previously described in a lung epithelial cell line (C10) or mouse lungs after inhalation of crocidolite asbestos (28), increases in expression of the early response gene, *FOSB*, that encodes a dimer of the activator protein-1 transcription factor, were seen. Increases in expression of several other genes linked to cell signaling proteins and transcription factor activation were observed in asbestos-exposed cells, including *NR4A2* and *PDK4*. A novel gene up-regulated at all time points and concentrations of asbestos or talc in human mesothelial cells was activating transcription factor 3 (*ATF3*), a member of the cAMP-responsive element–binding (CREB) transcription factor family that encodes two different isoforms leading to repression or activation of genes. Silencing of *ATF3* in the present study by siRNA significantly altered expression of a number of asbestos-induced inflammatory cytokines and growth factors documented in malignant mesotheliomas (29, 30). In support of our results here, other studies using *ATF3*-deficient mice and *in vitro* approaches have shown that *ATF3* is a negative regulator of pulmonary inflammation, eosinophilia, and airway responsiveness (31). Moreover, *ATF3* also negatively regulates IL-6 gene transcription in an NF-κB model of up-regulation using melanoma cells (32). In addition, trends in production of VEGF, a known important angiogenic peptide and independent prognostic factor in human mesotheliomas (33), were observed. We have recently shown that an extracellular signal–related

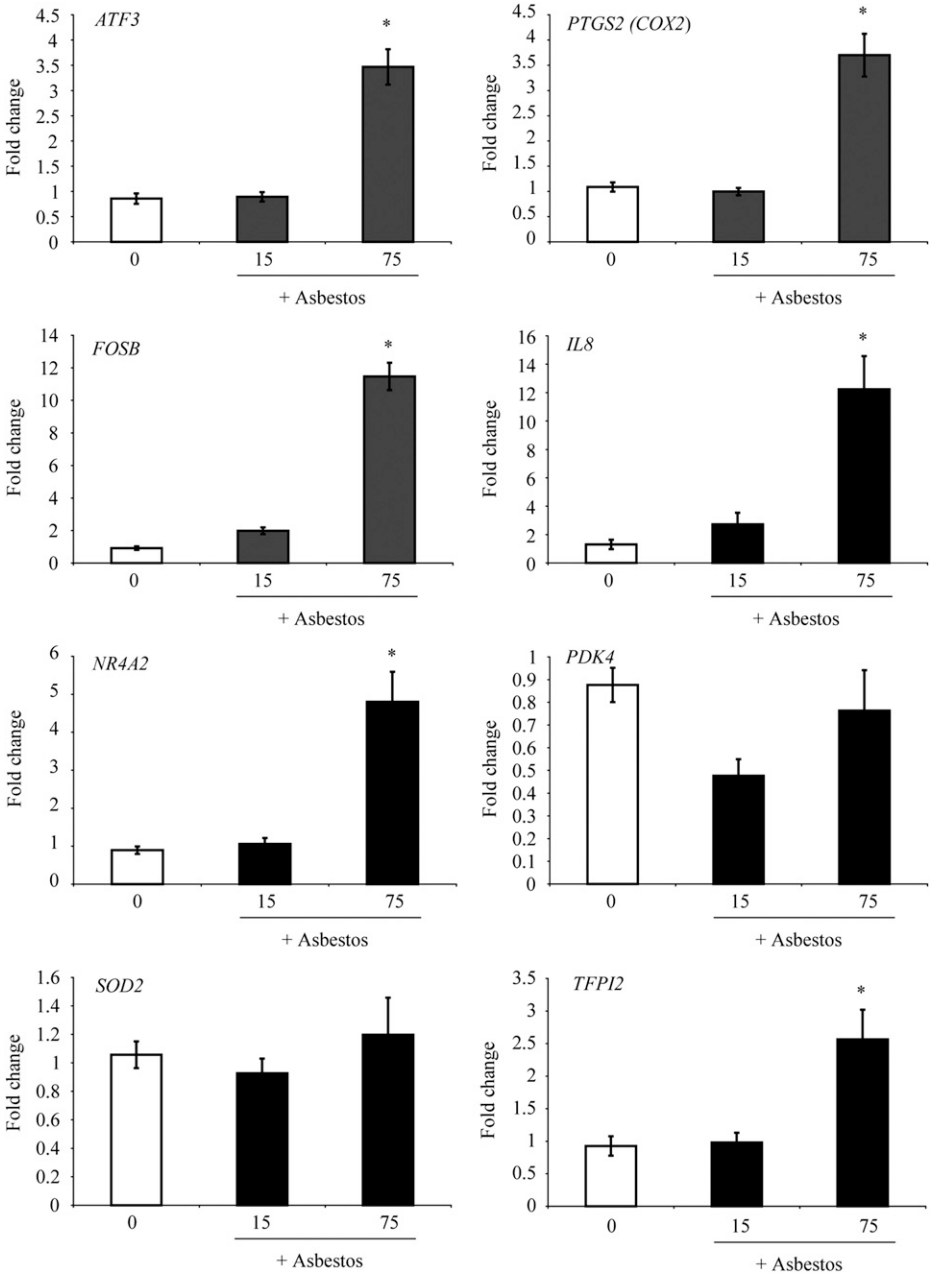

Figure 5. QRT-PCR confirms that human primary pleural mesothelial cells (NYU474) show similar patterns of asbestos-induced gene expression when compared with LP9/TERT-1 mesothelial cells. NYU474 cells were exposed to crocidolite asbestos (15 or 75 $\mu m^2/cm^2$) for 24 hours and cDNA was used for QRT-PCR. *$P \leq 0.05$ as compared with untreated cells (0).

CREB pathway in C10 lung epithelial cells modulates apoptosis after asbestos exposure (34), and recent studies are focusing on the effects of silencing *CREB* or *ATF3* on other functional and phenotypic changes in human mesothelial and mesothelioma cells (A. Shukla and colleagues, unpublished data).

Several other genes up-regulated by talc at 8 hours or affected by asbestos at both 8 and 24 hours may be important in repair from mineral-induced responses. For example, *SOD2*, (Mn-containing superoxide dismutase) is an antioxidant protein occurring in the mitochondria, a target cell organ of asbestos-induced apoptosis (35). *PTGS2* (prostaglandin-endoperoxide syntase or cyclooxygenase) is a key enzyme in prostenoid biosynthesis associated with modulation of mitogenesis and inflammation. More recently, this pathway has been explored after interaction of ultrafine particles with alveolar macrophages (9). *ANG PTL4* (angiopoietin-4) encodes a serum hormone directly involved in regulating glucose homeostasis and lipid metabolism and is an apoptosis survival factor for vascular endothelial cells. The up-regulation of angiopoietin-4 is also thought to play a role in inhibition of tumor cell motility and metastasis. *KLF4* (Kruppel-like factor 4) is a negative regulator of cell proliferation and can be a positive or negative modulator of DNA transcription.

Increased expression of genes encoding different cytokines/chemokines (i.e., *IL8*) and their receptors or ligands (e.g., IL-8 C-terminal variant, *IL1R1*, *CXCL2* or *MIP2*, *CXCL3*, and *TFP12*) by asbestos or talc suggests that the mesothelial cell also may play a role in chemotaxis, inflammation, and blood coagulation. A number of gene expression changes by asbestos also support the hypothesis that this fibrous mineral affects calcium-dependent processes including related protein kinase cascades, cell adhesion, and protein/lipid metabolism (Table 2). Although numbers of changes were more modest in IOSE cells, with the exception of *NR4A2* and *CXCL2*, a unique subset of genes was induced by asbestos in this cell type (Table 4).

Results of work here suggest that transcriptional profiling can be used to reveal molecular events by mineral dusts that are

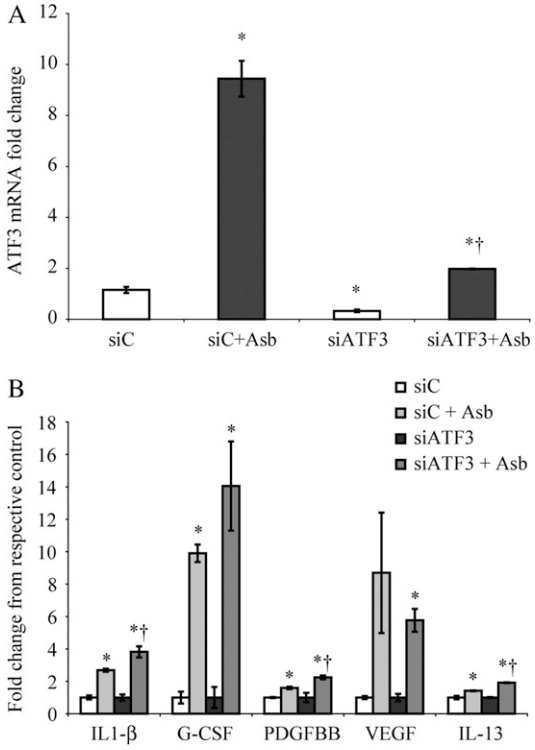

Figure 6. *ATF3* inhibition using siRNA approaches alters asbestos-induced production of inflammatory cytokines and growth factors. (*A*) LP9/TERT-1 cells transfected with siATF3 show significant inhibition of *ATF3* mRNA levels (untreated control [siC] versus siATF3 and asbestos-treated [siC Asb versus siATF3 Asb] groups). *$P \leq 0.05$ as compared with siC; †$P \leq 0.05$ as compared with siC Asb group. (*B*) siATF3 altered asbestos-induced cytokine levels as detected in medium at 24 hours using Bio-Plex analyses. *$P \leq 0.05$ as compared with control groups (siC and siATF3), respectively; †$P \leq 0.05$ as compared with asbestos-exposed scrambled control group (siC).

predictive of their pathogenicity in mesothelioma. Moreover, they reveal early and novel gene responses, including calcium-dependent transcription factors and antioxidant enzymes that may be pursued for their functional significance using RNA silencing or other approaches.

Conflict of Interest Statement: B.T.M. received support by EUROTALC and The Industrial Minerals Association (IMA) (11/1/05–10/31/06) for $90,000 for research. None of the other authors has a financial relationship with a commercial entity that has an interest in the subject of this manuscript.

Acknowledgments: The authors thank the Vermont Cancer Center DNA Analysis Facility for performing oligonucleotide microarray and real-time quantitative PCR, and Gary Tomiano (Minteg International, Inc./Specialty Minerals, Inc., Easton, PA) for talc characterization.

References

1. Mossman BT, Gee JB. Asbestos-related diseases. *N Engl J Med* 1989; 320:1721–1730.
2. Mossman BT, Churg A. Mechanisms in the pathogenesis of asbestosis and silicosis. *Am J Respir Crit Care Med* 1998;157:1666–1680.
3. Robinson BW, Lake RA. Advances in malignant mesothelioma. *N Engl J Med* 2005;353:1591–1603.
4. Mossman BT, Bignon J, Corn M, Seaton A, Gee JB. Asbestos: scientific developments and implications for public policy. *Science* 1990;247: 294–301.
5. Dickson MA, Hahn WC, Ino Y, Ronfard V, Wu JY, Weinberg RA, Louis DN, Li FP, Rheinwald JG. Human keratinocytes that express hTERT and also bypass a p16(INK4a)-enforced mechanism that limits life span become immortal yet retain normal growth and differentiation characteristics. *Mol Cell Biol* 2000;20:1436–1447.
6. Choi JH, Choi KC, Auersperg N, Leung PC. Overexpression of follicle-stimulating hormone receptor activates oncogenic pathways in pre-neoplastic ovarian surface epithelial cells. *J Clin Endocrinol Metab* 2004;89:5508–5516.
7. Merritt MA, Green AC, Nagle CM, Webb PM. Talcum powder, chronic pelvic inflammation and NSAIDs in relation to risk of epithelial ovarian cancer. *Int J Cancer* 2008;122:170–176.
8. Mossman BT, Shukla A, Fukagawa NK. Highlight Commentary on "Oxidative stress and lipid mediators induced in alveolar macrophages by ultrafine particles". *Free Radic Biol Med* 2007;43:504–505.
9. Beck-Speier I, Dayal N, Karg E, Maier KL, Schumann G, Schulz H, Semmler M, Takenaka S, Stettmaier K, Bors W, *et al.* Oxidative stress and lipid mediators induced in alveolar macrophages by ultrafine particles. *Free Radic Biol Med* 2005;38:1080–1092.
10. Oberdorster G, Ferin J, Gelein R, Soderholm SC, Finkelstein J. Role of the alveolar macrophage in lung injury: studies with ultrafine particles. *Environ Health Perspect* 1992;97:193–199.
11. Brown DM, Wilson MR, MacNee W, Stone V, Donaldson K. Size-dependent proinflammatory effects of ultrafine polystyrene particles: a role for surface area and oxidative stress in the enhanced activity of ultrafines. *Toxicol Appl Pharmacol* 2001;175:191–199.
12. Donaldson K, Tran CL. Inflammation caused by particles and fibers. *Inhal Toxicol* 2002;14:5–27.
13. Health Effects Institute - Asbestos Research. Asbestos in public and commercial buildings: a literature review and synthesis of current knowledge. Cambridge, MA: The Health Effects Institute; 1991.
14. Sabo-Attwood T, Ramos-Nino M, Bond J, Butnor KJ, Heintz N, Gruber AD, Steele C, Taatjes DJ, Vacek P, Mossman BT. Gene expression profiles reveal increased mClca3 (Gob5) expression and mucin production in a murine model of asbestos-induced fibrogenesis. *Am J Pathol* 2005;167:1243–1256.
15. Campbell WJ, Huggins CW, Wylie AG. Chemical and physical characterization of amosite, chrysotile, crocidolite, and nonfibrous tremolite for oral ingestion studies Washington, DC: National Institute of Environmental Health Sciences; 1980. No. 8542.
16. Blumen SR, Cheng K, Ramos-Nino ME, Taatjes DJ, Weiss DJ, Landry CC, Mossman BT. Unique uptake of acid-prepared mesoporous spheres by lung epithelial and mesothelioma cells. *Am J Respir Cell Mol Biol* 2007;36:333–342.
17. Shukla A, Lounsbury KM, Barrett TF, Gell J, Rincon M, Butnor KJ, Taatjes DJ, Davis GS, Vacek P, Nakayama KI, *et al.* Asbestos-induced peribronchiolar cell proliferation and cytokine production are attenuated in lungs of protein kinase C-delta knockout mice. *Am J Pathol* 2007;170:140–151.
18. Steiner G, Suter L, Boess F, Gasser R, de Vera MC, Albertini S, Ruepp S. Discriminating different classes of toxicants by transcript profiling. *Environ Health Perspect* 2004;112:1236–1248.
19. Lechner JF, Tokiwa T, LaVeck M, Benedict WF, Banks-Schlegel S, Yeager H Jr, Banerjee A, Harris CC. Asbestos-associated chromosomal changes in human mesothelial cells. *Proc Natl Acad Sci USA* 1985;82:3884–3888.
20. Nymark P, Lindholm PM, Korpela MV, Lahti L, Ruosaari S, Kaski S, Hollmen J, Anttila S, Kinnula VL, Knuutila S. Gene expression profiles in asbestos-exposed epithelial and mesothelial lung cell lines. *BMC Genomics* 2007;8:62.
21. Cacciotti P, Barbone D, Porta C, Altomare DA, Testa JR, Mutti L, Gaudino G. SV40-dependent AKT activity drives mesothelial cell transformation after asbestos exposure. *Cancer Res* 2005;65:5256–5262.
22. Davis JM, Addison J, Bolton RE, Donaldson K, Jones AD, Smith T. The pathogenicity of long versus short fibre samples of amosite asbestos administered to rats by inhalation and intraperitoneal injection. *Br J Exp Pathol* 1986;67:415–430.
23. Stanton MF, Layard M, Tegeris A, Miller E, May M, Morgan E, Smith A. Relation of particle dimension to carcinogenicity in amphibole asbestoses and other fibrous minerals. *J Natl Cancer Inst* 1981;67:965–975.
24. Guthrie GD Jr, Mossman BT. Health effects of mineral dusts. Washington, DC: Mineralogical Society of America; 1993.
25. IARC. Silica and some silicates. *IARC Monogr Eval Carcinog Risk Chem Hum* 1987;42:185.
26. Mossman B, Light W, Wei E. Asbestos: mechanisms of toxicity and carcinogenicity in the respiratory tract. *Annu Rev Pharmacol Toxicol* 1983;23:595–615.
27. Janssen YM, Heintz NH, Mossman BT. Induction of c-fos and c-jun proto-oncogene expression by asbestos is ameliorated by N-acetyl-L-cysteine in mesothelial cells. *Cancer Res* 1995;55:2085–2089.

28. Ramos-Nino ME, Heintz N, Scappoli L, Martinelli M, Land S, Nowak N, Haegens A, Manning B, Manning N, MacPherson M, *et al.* Gene profiling and kinase screening in asbestos-exposed epithelial cells and lungs. *Am J Respir Cell Mol Biol* 2003;29:S51–S58.
29. Yoshimoto A, Kasahara K, Saito K, Fujimura M, Nakao S. Granulocyte colony-stimulating factor-producing malignant pleural mesothelioma with the expression of other cytokines. *Int J Clin Oncol* 2005;10:58–62.
30. Vogelzang NJ, Herndon JE II, Miller A, Strauss G, Clamon G, Stewart FM, Aisner J, Lyss A, Cooper MR, Suzuki Y, *et al.* High-dose paclitaxel plus G-CSF for malignant mesothelioma: CALGB phase II study 9234. *Ann Oncol* 1999;10:597–600.
31. Gilchrist M, Henderson WR Jr, Clark AE, Simmons RM, Ye X, Smith KD, Aderem A. Activating transcription factor 3 is a negative regulator of allergic pulmonary inflammation. *J Exp Med* 2008;205:2349–2357.
32. Karst AM, Gao K, Nelson CC, Li G. Nuclear factor kappa B subunit p50 promotes melanoma angiogenesis by upregulating interleukin-6 expression. *Int J Cancer* 2009;124:494–501.
33. Demirag F, Unsal E, Yilmaz A, Caglar A. Prognostic significance of vascular endothelial growth factor, tumor necrosis, and mitotic activity index in malignant pleural mesothelioma. *Chest* 2005;128: 3382–3387.
34. Barlow CA, Barrett TF, Shukla A, Mossman BT, Lounsbury KM. Asbestos-mediated CREB phosphorylation is regulated by protein kinase A and extracellular signal-regulated kinases 1/2. *Am J Physiol Lung Cell Mol Physiol* 2007;292:L1361–L1369.
35. Shukla A, Stern M, Lounsbury KM, Flanders T, Mossman BT. Asbestos-induced apoptosis is protein kinase C delta-dependent. *Am J Respir Cell Mol Biol* 2003;29:198–205.